β-Catenin Upregulates the Constitutive and Virus-Induced Transcriptional Capacity of the Interferon Beta Promoter through T-Cell Factor Binding Sites.

Vasco Marcato, Lionel Luron, Lucie M Laqueuvre, Dominique Simon, Zeyni Mansuroglu, Marie Flamand, Jean-Jacques Panthier, Sylvie Souès, Charbel Massaad, Eliette Bonnefoy

HAL Id: pasteur-01326511
https://pasteur.hal.science/pasteur-01326511

Submitted on 3 Jun 2016

1 **Beta-catenin up-regulates the constitutive and virus-induced transcriptional capacity of**

2 **the interferon-β promoter through T-cell factor binding sites**

3

4 Vasco Marcato[1], Lionel Luron[1], Lucie M. Laqueuvre[1], Dominique Simon[3,4], Zeyni

5 Mansuroglu[1], Marie Flamand[2], Jean-Jacques Panthier[3,4], Sylvie Souès[1], Charbel Massaad[5] &

6 Eliette Bonnefoy[1#]

7

8 [1]Inserm UMR-S1007, Université Paris Descartes, Sorbonne Paris Cité, Paris, France; [2]Institut

9 Pasteur, Unité de Recherche de Virologie Structurale, Paris, France; [3]Institut Pasteur, Unité

10 de Génétique Fonctionnelle de la Souris, Paris, France; [4]Centre National de la Recherche

11 Scientifique URA 2578, Paris, France; [5]Inserm UMR-S1124, Université Paris Descartes,

12 Sorbonne Paris Cité, Paris, France.

13

14 Running title: TCF/β-catenin regulation of IFN-β gene expression

15

16 Word count for abstract : 192

17 Word count for text : 6116

18 Word count for Materials and Methods: 1032

19

20 [#]corresponding author: eliette.bonnefoy@parisdescartes.fr

21

22   **Abstract**

23   Rapid up regulation of interferon-β (IFN-β) expression following virus infection is essential

24   to set up an efficient innate antiviral response. Biological roles related to the antiviral and

25   immune response have also been associated to the constitutive production of IFN-β in naïve

26   cells. However, mechanisms capable to modulate constitutive IFN-β expression in the

27   absence of infection remain largely unknown. In this work we demonstrate that inhibition of

28   kinase GSK-3 leads to the up-regulation of the constitutive level of IFN-β expression in non-

29   infected cells, provided that GSK-3 inhibition be correlated with binding of β-catenin to the

30   IFN-β promoter. Under these conditions, IFN-β expression occurred through the T-cell factor

31   (TCF) binding sites present on the IFN-β promoter, independently of IRF3. Enhancement of

32   the constitutive level of IFN-β was *per se* capable to confer an efficient antiviral state to naïve

33   cells and acted in synergy with virus infection to stimulate virus-induced IFN-β expression.

34   Further emphasizing the role of β-catenin in the innate antiviral response, we show here that

35   highly pathogenic Rift Valley fever virus (RVFV) targets the Wnt/β-catenin pathway and the

36   formation of active TCF/β-catenin complexes at the transcriptional and protein level in

37   RVFV-infected cells and mice.

38

Introduction

40   Production of interferon-β (IFN-β) plays a central role in the induction of the innate

41   antiviral response (1,2). Rapid up-regulation of IFN-β gene expression occurs after

42   recognition of viral nucleic acids by pattern recognition receptors (PRRs) either cytosolic

43   such as retinoic acid-inducible gene I (RIG-I) and melanoma differentiation-associated

44   antigen 5 (MDA-5) or membrane-associated Toll-like receptors such as TLR3 (3). After

45   sensing single or double stranded RNA of viral origin, these receptors activate signaling

46   pathways implicating the phosphorylation and nuclear translocation of several transcription

47   factors among which the interferon regulatory factor 3 (IRF3), rapidly leading downstream to

48   a robust activation of the expression of IFN-β gene. After being secreted, IFN-β protein binds

49   to the type I interferon receptor and triggers the JAK-STAT1/2 signal transduction pathway.

50   This pathway leads to the activation and inhibition of the expression of a large set of genes

51   that constitute the type I IFN response mounted to antagonize viral infection at different levels

52   (4).

53   Mice lacking IFN-β (5) or the subunit of the type I interferon receptor (6,7) are highly

54   susceptible to viral infections. They succumb to sub-lethal doses of a variety of viruses thus

55   confirming the main role of IFN-β in the establishment of an innate antiviral response.

56   However, beyond the antiviral response, IFN-β affects a wide range of other biological

57   functions for the most related to modulation of the immune (innate and adaptive) and

58   inflammatory responses as well as to cell proliferation and differentiation. Even though IFN-β

59   has been described of anti-inflammatory benefit, it has also been implicated in the

60   development of several inflammatory and autoimmune diseases (8-10). Hence, the beneficial

61   or detrimental outcome of IFN-β expression for the organism will depend on the timing, the

62   kinetics and the amount of IFN-β being synthesized (11,12). If a marked activation of IFN-β

63   gene expression is required to efficiently set up the appropriate response to an external

64   aggression such as virus infection, this response needs to be adjusted in order to limit its

65   pathological side effects.

66   As expected for a gene with pleiotropic functions, its transcriptional state is regulated

67   at different levels. At the cellular level, only a stochastic fraction of the infected cells produce

68   IFN-β (13,14) as a way to avoid an exacerbated and uncontrolled IFN response. At the

69   nuclear level, one IFN-β allele localizes within interchromosomal regions rich in NF-κB

70   DNA binding sites before and after infection (15) whereas the other allele localizes next to

71   pericentromeric heterochromatin (PCH) clusters in the absence of infection and dissociates

72   from PCH clusters during infection (16). The monoallelic characteristic of these particular

73   subnuclear localizations suggests that a yet non-deciphered regulatory mechanism exists at

74   the chromosome level. Finally, at the promoter level, the coordinated action of several

75   transcription factors and chromatin remodeling complexes (17-21) regulate the IFN-β

76   promoter transcriptional capacity. Among transcription factors, IRF3 plays an essential role

77   during pathogen dependent activation of IFN-β gene expression in most cell types (22).

78   Alongside with IRF3, are recruited over the promoter transcription factors such as NF-κB

79   (15,23), ATF2/c-Jun and YY1 (20,24,25) that participate in the recruitment of chromatin

80   remodeling complexes associated with histone acetyltransferase CBP. Some of these factors

81   play dual roles, acting not only as activators but also as repressors of IFN-β expression. This

82   is the case for NF-kB (26) and YY1 (27). Specially, YY1 participates in the transcriptional

83   activation through recruitment of CBP and in the establishment of the repressive state of the

84   IFN-β promoter through recruitment of co-repressor SAP30 (21) and association with

85   pericentromeric heterochromatin (16).

86   Even though the IFN-β gene has been considered as repressed in naïve cells, low

87   levels of IFN-β have been detected in different types of non-infected cells in the central

88   nervous system (28,29), splenocytes and mouse embryonic fibroblasts (MEFs) (30) implying

89   the existence of mechanisms capable to regulate the production of limited amounts of IFN-β

90   in the absence of infection. Using anti-IFN-α/β antibodies, Haller et al. (31) evidenced a role

91   of such IFN-β production with respect to the establishment of an active antiviral response.

92   Using a similar strategy, Vogel and Fertsch (32) showed that the IFN-β production detected in

93   non-infected cells had an autostimulatory role upon macrophage differentiation. More

94   recently, results obtained with mice lacking either IFN-β or its receptor have confirmed the

95   physiological role of such low amounts of IFN-β produced by non-infected animals in

96   relation with several biological functions such as immune cell function, antiviral defense,

97   bone remodeling and modulation of homeostatic balance (reviewed in 33). As in the case of

98   virus-induced IFN-β production, deregulation of virus-independent IFN-β expression can lead

99   to pathological effects. However, mechanisms capable to affect IFN-β expression in the

100 absence of infection remain to be clarified.

101   In the cytoplasm, β-catenin is found within a degradation complex associated with

102 Adenomatous Polyposis Coli (APC), Axin and GSK-3 as well as CK1A Ser/Thr kinases that

103 control the level of free β-catenin by a phosphorylation-dependent targeting of β-catenin

104 towards proteasome degradation (34,35). Disruption of the degradation complex through

105 inhibition of GSK-3 kinase leads to the increase of β-catenin and its subsequent nuclear

106 accumulation. In the nucleus, β-catenin physically interacts with T-cell factor (TCF) to

107 regulate the expression of target genes through the recruitment of a transcriptional activator

108 complex containing B-Cell Lymphoma 9 (BCL9) protein and CBP over promoter regions

109 carrying binding sites for TCF factors (36-38).

110   With the goal to identify mechanisms susceptible to affect the level of IFN-β

111 expression in the absence of infection, namely IRF3-NFκB-ATF2/cJUN-independent

112 expression considered here as constitutive expression, we have questioned in this work the

5

113   capacity of nuclear β-catenin to regulate IFN-β expression, in naïve and infected cells, in

114   association with the TCF family of transcription factors for which we show that DNA binding

115   sites are present in the murine and human IFN-β promoter.

116   We demonstrate here that LiCl treatment, a potential inhibitor of GSK-3, enhanced the

117   constitutive level of IFN-β expression provided that it would lead to the interaction of β-

118   catenin with IFN-β promoter. While it has been previously reported that β-catenin would

119   modulate IFN-β expression either positively (39-43) or negatively (44) through IRF3, our

120   results uncover a new mechanism of up-regulation of the transcriptional capacity of the IFN-β

121   promoter following LiCl treatment mediated by TCF/β-catenin complexes recruited over the

122   IFN-β promoter region. Moreover, we show that the up-regulation of the constitutive level of

123   IFN-β expression following LiCl treatment leads to the establishment of an efficient antiviral

124   state protecting naïve cells against virus-induced cytopathic effect and acts in synergy with

125   infection to increase IFN-β production. Further emphasizing the importance of TCF/β-catenin

126   complex formation in the antiviral response, we show here that the pathogenicity induced by

127   Rift Valley fever virus (RVFV) infection of cell cultures and mice was correlated with viral

128   targeting of the TCF/β-catenin pathway at different levels.

129

Materials and Methods

131 **Virus, Cells and Mice**

132   Stocks of RVFV ZH548 and RVFV ZHΔNSs were produced under BSL3 conditions

133 by infecting Vero cells at m.o.i. of 10^{-3} and by harvesting the medium at 72 hr p.i. Murine

134 fibroblastic L929 cell line and NDV infections were described previously (45). Murine

135 hepatocyte AML12 cell line was from ATCC (ref. CRL-2254). For preparation of bone

136 marrow-derived macrophages (BMDM) preparation, bone marrow from tibiae and femora of

137 8-12 weeks B6 mices was flushed and cultured for 7 days in DMEM containing 10% heat-

138 inactivated fetal bovine serum, 100 U/ml penicillin/streptomycin, 2 mM glutamine and 10

139 ng/ml murine M-CSF (Peprotech). Infection of mice was performed as previously described

140 (46). When indicated, LiCl, iCRT3 (Sigma) or LiCl+iCRT3 were directly added to the culture

141 medium.

142

143 **Antibodies**

144   Mouse anti-NSs and rabbit anti-N polyclonal antibodies were raised respectively

145 against the entire NSs or N protein (47). Anti-β-catenin from BD Transduction laboratories

146 (Cat#610154) was used for immunofluorescence, Western blot and gel retardation. Secondary

147 antibodies used for immunofluorescence were Alexa 488 fluor-conjugated chicken anti-

148 mouse from Invitrogen (A21200) and Alexa 555 fluor-conjugated donkey anti-rabbit from

149 Invitrogen (A31572). Secondary antibodies used for Western blot were ECL Mouse IgG,

150 HRP-linked whole Ab (NA931) an ECL Rabbit IgG, HRP-linked whole Ab (NA934) from GE

151 Healthecare Life Sciences.

152

153   **Immunofluorescence**

154   For immunofluorescence, cells grown in 6-well plates on coverslips were fixed with

155   4% formaldehyde in PBS for 15 minutes and permeabilized with 1% Triton X-100 in PBS for

156   20 minutes. Then cells were incubated for 1 hour at room temperature with the corresponding

157   primary antibodies diluted in PBS/BSA 5%. Cells were then washed with PBS and incubated

158   for 1 hour at room temperature with corresponding secondary antibodies.

159

160   **Image acquisition and manipulation**

161   Samples were analyzed at room temperature by confocal laser scanning microscopy

162   using a Zeiss LSM710 confocal system at the *Service Commun de Microscopie* (SCM) of

163   Université Paris Descartes. This system is equipped with a 63x, 1.4 O.N oil immersion lens

164   (Plan Neofluor). For oil immersion microscopy, we used oil with refractive index of 1.518

165   (Zeiss). Image capture was carried out with a definition of 1024x1024 pixels with 8 bit data

166   for each color. Images were analyzed using Image J software. Total pixel intensity was

167   quantified using Image J software.

168

169   **Chromatin immunoprecipitation**

170   Chromatin immunoprecipitation experiments were carried out as previously described (21).

171   PCR analysis of inputs or immunoprecipitated DNAs was performed using oligonucleotides

172   F-40 (5'-GTT TTC CCA GTC ACG AC-3') and CAT (5'-CCA TTT TAG CTT CCT TAG-

173   3') to reveal the integrated WT330 and WT110 IFN-β promoter. For the F-40, CAT set of

174   primers, PCR conditions were as follows: 1 cycle of 94°C for 5 minutes; 20 cycles of 94°C

175   for 30 seconds, 53°C for 30 seconds and 72°C for 30 seconds; 1 cycle of 72 °C for 10

176   minutes. A first "cold" PCR was carried out in the presence of 25 pmol of each primer; 1.5 µl

177   of the product of the first PCR was subjected to a second "hot" PCR carried out in the

178   presence of 0.1 µl a-^{32}PdATP (6000 Ci/mmol) and 25 pmol of each primer.

179

180   **RT-qPCR**

181   Total RNA was extracted using Tri Reagent (Sigma) according to the manufacturer's

182   protocol. 1 µg of total RNA was reversely transcribed using High Capacity cDNA Reverse

183   Transcription Kit (Applied Biosystems) according to the manufacturers' recommendations

184   using Random Primers. qPCR was performed using SYBR Green (Thermo Scientific)

185   reagents: 95°C 15 minutes, then 40 cycles at 95°C 15 seconds, 60°C 1 minute, followed by a

186   dissociation step. Relative quantification of mRNA expression was calculated using the $\Delta\Delta C_T$

187   method using three reference genes among Ppib, Hprt1, Utp6c and Rplp0). For fold changes

188   lower than 1 (translating a repression of the gene's expression), the inverted values were

189   determined such that a 0.5 fold change corresponds to -2. Sequences of primers used for RT-

190   qPCR analysis are shown in Table I.

191   Statistical analysis was carried out using Student T-test or the REST software that uses a Pair-

192   Wise Fixed Reallocation Randomization Test© to determine a P-value.

193

194   **RNA interference experiments**

195   L929 cells were transfected using Lipofectamine 2000 (Invitrogen Life Technologies)

196   with the ON Target Plus SMART Pool of siRNA oligos specific for β-catenin (Thermo

197   Scientific Dharmacon® L-040628-00) or with a pool of control siRNA sequences (Thermo

198   Scientific Dharmacon® D-001810-10-05) at a final concentration of 50nM each during 72 h.

199

200

201

202 **Gel retardation assay**

203   Nuclear extracts of murine L929 cells either non-treated or treated with LiCl for 24 h

204 were incubated with the corresponding 5' ^{32}P-labeled probes in 20 µl (final volume) of 50

205 mM Tris-HCl (pH 7.5), 50 mM NaCl, 5 mM EDTA, 10% glycerol and 5 mM dithiothreitol.

206 When indicated, anti-β-catenin antibody was incubated with the nuclear extracts 1 h at 4°C

207 prior to the addition of the labeled probe.

208

209 **Cytopathic effect assays.**

210   Monolayer cultures of L929 cells in 96-well plates were incubated with LiCl for 24 h

211 before VSV infection. Before VSV infection, the medium containing LiCl was removed.

212 Viruses were diluted in medium with serum (2% final concentration) and added directly to the

213 culture medium. The monolayers were stained with crystal violet as vital dye 24 h after VSV

214 infection or fixed 8h after VSV infection for immunofluorescence analysis. For measurement

215 of the cytopathic effet of RVFV, L929 cells either non-treated or treated with LiCl for 24 h

216 were infected with RVFVZH548 and incubated under an overlay consisting of DMEM, 2%

217 fetal calf serum, antibiotics and 1% agarose at 37°C. At 3 day p.i., the lytic plaques were

218 counted after staining with a solution of crystal violet.

219

220 **Western blot**

221   For Western blot, total protein extracts were prepared in RIPA buffer and resolved by

222 sodium dodecyl sulfate-polyacrylamide gel electrophoresis (SDS-PAGE) in 4-12% precast

223 gels (Life Technologie). Relative quantification of proteins was carried out using Image

224 Quant software on scanned WB films.

225

226 **Ethics Statement**

10

227   Experiments on live mice were conducted according to the French and European

228   regulations on care and protection of laboratory animals (EC Directive 86/609, French Law

229   2001-486 issued on June 6, 2001) and the National Institutes of Health Animal Welfare

230   (Insurance #A5476-01 issued on 02/07/2007). Experimental protocols were approved by the

231   Animal Ethics Committee #1 of the *Comité Régional d'Ethique pour l'Expérimentation*

232   *Animale* (CREEA), Ile de France (N°2012-0025), and carried out in compliance with Institut

233   Pasteur Biosafety Committee.

234

Results

LiCl treatment enhances constitutive IFN-β gene expression.

237   The proximal region of the IFN-β promoter (Fig. 1A), made of negative and positive

238   regulatory domains, is highly conserved between murine and human cells. The Virus

239   Responsive Element (VRE) that contains binding sites for transcription factors IRF3, ATF2/c-

240   Jun, NF-κB and YY1 is surrounded by two Negative Regulatory Domains (NRDI and II)

241   described as regions of nucleosome positioning (18). Sequence analysis of the murine IFN-β

242   promoter revealed the presence in the NDRII of two potential DNA-binding sequences for

243   TCF transcription factors. A first site, TCFa, between positions -374 and -367 (5'-

244   TTCAAAGG-3') that perfectly matches the consensus TCF DNA binding sequence 5'-

245   (A/T)(A/T)CAAAGG-3' (38). A second site, TCFb, between positions -233 and -226 (5'-

246   CCTTTGcT-3') that differs from the consensus TCF DNA binding sequence by one base.

247   Two sequences homologous to the murine TCFb sequence are present in the human IFN-β

248   promoter, between positions -260 and -253 and +26 and +33 respectively.

249   The presence of potential TCF binding sites within the proximal region of the IFN-β

250   promoter suggested that expression of the IFN-β gene could be modulated in response to

251   pathways inducing nuclear accumulation of β-catenin and formation of TCF/β-catenin

252   complexes over the IFN-β promoter region. In order to test this hypothesis, we analyzed IFN-

253   β gene expression in non-infected cells, corresponding to an IRF3-NF-κB-ATF2/c-Jun

254   independent expression that we have considered as constitutive IFN-β expression, before and

255   after nuclear accumulation of β-catenin. Experiments were carried out in murine fibroblastic

256   L929 cells, which are potent IFN-β producer cells. In the absence of GSK-3 inhibition, little if

257   any β-catenin was detected in the nucleus of L929 cells whereas the nuclear distribution of β-

258   catenin was significantly enhanced after treatment of the cells with LiCl, an inhibitor of GSK-

259   3 (Fig. 1B-D). IFN-β gene expression measured by RT-qPCR in LiCl-treated cells compared

260   to untreated cells, showed that LiCl treatment significantly enhanced the constitutive level of

261   IFN-β mRNAs ($p<10^{-5}$) (Fig. 1E) independently of any virus infection. Even though the level

262   of IFN-β expression measured after LiCl treatment was much lower than that induced during

263   viral infection (16), it was sufficient to trigger an IFN-β response as reflected by a significant

264   induction of the expression of two major IFN-stimulated genes (ISGs), *Oas1b* and *Irf7* genes

265   (Fig. 1F). The effect of LiCl on IFN-β expression was dose dependent. The highest effect,

266   before reaching saturation, was observed at 20 mM LiCl (Fig. 1G).

267   Low constitutive levels of IFN-β have been previously shown to synergize with virus

268   infection for efficient virus-induced IFN-β production (30,48). In order to test if the

269   enhancement of the constitutive level of IFN-β gene expression induced by LiCl in naïve cells

270   could affect virus induced IFN-β expression, L929 cells were either pretreated or not with

271   LiCl before being infected with Newcastle Disease Virus (NDV) that, contrary to LiCl, does

272   not induce the nuclear accumulation of β-catenin (Fig. 1H and J). As shown in Fig. 1J,

273   pretreatment of the cells with LiCl significantly potentiated NDV-induced IFN-β expression.

274

275   **The effect of LiCl treatment on IFN-β expression is mediated by β-catenin.**

276   In order to confirm that the effect of LiCl treatment on constitutive IFN-β expression

277   was not due to LiCl treatment *per se* but required the nuclear accumulation of β-catenin, we

278   made use of murine hepatocyte AML12 cells that produce IFN-β in response to viral infection

279   but, by contrast to L929 cells, do not accumulate nuclear β-catenin after LiCl treatment (Fig.

280   2A and B). Measurement of the expression of IFN-β mRNA in AML12 cells either treated or

281   not with LiCl, before (Fig. 2C) and after (Fig. 2D) NDV infection, showed that the inability

282   of LiCl to induce the accumulation of nuclear β-catenin in this particular cell type correlated

13

283 with the inability of LiCl treatment to enhance IFN-β expression either in the absence

284 (Fig.2C) or presence (Fig. 2D) of virus infection.

285 The role of β-catenin during LiCl enhancement of IFN-β expression was further

286 confirmed using siRNAs. For this, L929 cells were mock-transfected or transfected either

287 with siRNAs directed against β-catenin or with control siRNAs (Fig. 2E-G) before being

288 treated with LiCl for 24h. Under conditions of diminution of β-catenin mRNA (Fig. 2E) and

289 protein (Fig. 2F) level, we observed that LiCl treatment had no significant effect on IFN-β

290 expression compared to cells treated with control siRNAs (Fig. 2G) confirming therefore that

291 the capacity of LiCl treatment to activate IFN-β expression was mediated by β-catenin.

292

293 **LiCl treatment stimulates the recruitment of β-catenin on the IFN-β promoter through**

294 **the NRDII promoter region containing a TCF binding site.**

295 IRF3 transcription factor is known to promote IFN-β expression, yet its activation,

296 nuclear translocation and subsequent IFN-β promoter binding, require the previous activation

297 of PRRs. The capacity of LiCl treatment to affect IFN-β gene expression in the absence of

298 infection showed that activation of the transcriptional capacity of the IFN-β promoter could

299 occur independently of IRF3, through a mechanism that we hypothesized to be TCF/β-

300 catenin-dependent. In order to test this hypothesis, we made use of previously established

301 L929 cell lines carrying integrated into their genome the proximal IFN-β promoter region

302 fused to the CAT reporter gene either from positions -330 to +20 (L929 WT330 cells) or from

303 positions -110 to +20 (L929 WT110 cells) (45). The NRDI region and the entire VRE region,

304 containing the IRF3 binding site, are present in both promoters whereas the NRDII region,

305 containing a TCF binding site, is only present on the WT330 promoter (Fig. 3A). Therefore,

306 contrary to the WT330 promoter that contains a TCF binding site, no TCF binding site is

307 present in promoter WT110.

14

308   ChIP analysis presented in Fig. 3B indicates that LiCl treatment induced β-catenin

309 binding to the WT330 promoter but not to the WT110 promoter, demonstrating that β-catenin

310 binding to the IFN-β promoter that occurred in the absence of virus infection required the

311 NRDII region containing a TCF binding site.

312   If, as hypothesized, the activation of IFN-β expression induced after LiCl treatment

313 required the recruitment of β-catenin on the IFN-β promoter, then only the WT330 promoter

314 was expected to respond to LiCl treatment. In order to test this prediction, we pretreated L929

315 WT330 and WT110 cells with LiCl and assayed the corresponding CAT activities (Fig. 3C).

316 As expected, LiCl treatment enhanced by 4-folds the constitutive transcriptional capacity of

317 the WT330 promoter, but not that of the WT110 promoter. Thus reinforcing the indispensable

318 role of the promoter region positioned 5' of the VRE, containing a TCF binding site, for LiCl

319 treatment to enhance the constitutive transcriptional capacity of the IFN-β promoter.

320   The role of the NRDII region containing a TCF binding site during LiCl-dependent

321 promoter activation was also analyzed after virus infection. As shown in Fig. 3D, LiCl

322 treatment enhanced the virus-induced activity of the WT330 promoter, but not that of the

323 WT110 promoter. Therefore, the presence of the NRDII region containing a TCF-binding site

324 was also required for the LiCl-dependent enhancement of the virus-induced transcriptional

325 capacity of the IFN-β promoter. The presence of only the VRE region, containing the IRF3

326 binding site (promoter WT110), was not sufficient to either recruit β-catenin or mediate LiCl

327 enhancement of the constitutive as well as virus-induced transcriptional capacity of the IFN-β

328 promoter.

329   LiCl that is considered as an inhibitor of GSK-3 can also affect the activity of other

330 kinases. In order to further investigate if the effect of LiCl on IFN-β expression was the

331 consequence of the inhibition of GSK-3, L929wt330 and wt110 cells were treated with two

332 other inhibitors of GSK-3, SB216763 and inhibitor IX. Similarly to LiCl, a dose dependent

15

333   activation of the transcriptional capacity of the WT330 promoter was observed in the

334   presence of increasing amounts of SB216763 (Fig. 3E). Also, treatment with either SB216763

335   or inhibitor IX had the same effect than LiCl, activating the transcriptional capacity of

336   WT330 promoter but not that of WT110 promoter (Fig. 2E and F). Since GSK-3 is a common

337   target for these three inhibitors, the fact that LiCl, SB216763, and inhibitor IX had the same

338   effect on the transcriptional capacity of the IFN-β promoter strongly supports the hypothesis

339   that LiCl dependent enhancement of IFN-β expression is the consequence of the inhibition of

340   GSK-3.

341

342   **The effect of LiCl treatment on IFN-β expression is mediated by TCF.**

343   Gel retardation assays were used to analyze the capacity of TCF binding sites present

344   within the NRDII region of IFN-β promoter to form complexes displaying the characteristics

345   of TCF-DNA complexes. For this, we used oligonucleotides containing the sequence of wild-

346   type, mutated TCFa or mutated TCF b sites. TCF binding sites were mutated in their core

347   motif containing the stretches of A required for the HMG box of TCF factors to interact with

348   DNA. The TCFa site was mutated to give rise to TCFmutA (5'-TTC*gg*AGG-3') site and the

349   TCFb site was mutated to give rise to TCFmutB (5'-CC*cc*TGcT-3') site. The corresponding

350   radioactively labeled, double-stranded DNA probes were incubated with nuclear extracts

351   prepared from L929 cells either non-treated or treated by LiCl during 24h. Whereas complex

352   formation was only weakly observed in the presence of nuclear extracts from non-treated

353   cells, a protein-DNA complex (indicated by an arrow in Fig. 4A) was clearly formed when

354   the DNA probes containing the wild-type TCFa or TCFb sites were incubated with nuclear

355   extracts from LiCl treated cells. As expected for a TCF-DNA complex, complex formation

356   was disrupted when the core region of the TCF DNA binding sequence was mutated as in

357   TCFmutA and mutB probes (Fig. 4B). T-Cell Factors interact with the minor groove of A/T

16

358   base pairs through their HMG-box and therefore are known to display affinity for I/C

359   sequences that resemble A/T sequences in the minor groove (49, 50). Therefore, as expected

360   for a TCF-DNA complex, the previous incubation of nuclear extracts with non-labeled

361   polydI/dC sequences inhibited complex formation with the radioactively labeled TCFA probe

362   (Fig. 4B). Finally, incubation of the nuclear extracts with anti-β-catenin antibodies affected

363   the formation of the protein-DNA complex that in the presence of antibodies was less intense

364   and supershifted (Fig. 4B), indicative of the presence of β-catenin within the complex.

365   To confirm the role of TCF binding sites in the LiCl dependent activation of the IFN-β

366   promoter transcriptional capacity, the IFN-β promoter region from positions -458 to +36

367   either wild-type or mutated in one or both TCF binding sites was cloned in front of the

368   luciferase reporter gene. After transfecting the corresponding plasmids into L929 cells, the

369   transfected cells were either treated or not with LiCl before being infected with NDV. The

370   corresponding luciferase activities were measured (Fig. 4C). Contrary to wild-type and mutB

371   promoters whose corresponding transcriptional capacities could be activated following LiCl

372   treatment, promoter mutA partially lost its capacity to be activated by LiCl and no activation

373   was observed in the case of the promoter mutAB. Therefore, results obtained here with TCF

374   mutated promoters demonstrated that the presence of at least one TCF binding site was

375   required for LiCl to activate the transcriptional capacity of the IFN-β promoter. In the context

376   of the promoter region cloned in these constructions (from -458 to +36), the TCFa that

377   perfectly matches the consensus sequence site appeared more efficient than the TCFb site.

378   In order to definitively confirm the role of TCF/β-catenin complexes during LiCl

379   enhancement of the transcriptional capacity of the endogenous IFN-β promoter, we used

380   iCRT3, which is a potent inhibitor of TCF4/β-catenin complexes (51). The presence of IFN-β

381   mRNAs was measured in NDV-infected L929 cells that were either non-treated or pretreated

382   with LiCl during 24 or 48 h in the absence or presence of different amounts of iCRT3

17

383   corresponding to the range of iCRT3 concentration necessary to inhibit TCF/β-catenin

384   dependent transcription of the Axin-2 and CycD1 (51). A dose-dependent inhibition of the

385   effect of LiCl on IFN-β expression was observed in the presence of iCRT3, and this in the

386   case of 24h as well as 48h (Fig. 4D) of LiCl treatment. In the same samples, iCRT3 also

387   inhibited the activation of the expression of the gene coding for CyclinD1 (Fig. 4E), which is

388   known to be regulated by TCF/β-catenin complexes. Overall demonstrating that the capacity

389   of LiCl to enhance IFN-β expression was mediated by TCF/β-catenin complexes.

390

391   **LiCl treatment confers an efficient antiviral response.**

392   Fig. 1E shows that LiCl-dependent enhancement of the constitutive level of IFN-β

393   expression was sufficient to lead to a significant activation of the expression of two major

394   ISGs, *Oas1b* and *Irf7*, responsible for the RNaseL-dependent degradation of viral ARN and

395   for the amplification of the IFN-β response respectively. In order to analyze the efficiency of

396   such LiCl-induced interferon response with respect to the establishment of an antiviral state,

397   we compared the cytopathic effect (CPE) of Vesicular Stomatitis Virus (VSV) in murine

398   L929 cells either pretreated or not with LiCl. Indeed, following infection of murine L929 cells

399   with VSV, cell viability is expected to decrease as the amount of VSV increases unless an

400   efficient IFN-β response had been mounted previously to VSV infection (52).

401   L929 cells pretreated or not with LiCl were infected with increasing titers of VSV.

402   Twenty-four hours after infection, the cells were stained with crystal violet, which detects

403   CPE as a decrease in staining intensity. As shown in Fig. 5A, at low multiplicity of infection

404   (MOI), cells pretreated with LiCl displayed less VSV-induced CPE than untreated cells,

405   highlighting the capacity of LiCl treatment to induce an efficient antiviral response protecting

406   cells against VSV-induced cell death. The capacity of LiCl treatment to confer an efficient

407   antiviral response at low MOI is further depicted in photographs of culture fields of LiCl-

18

408   treated versus untreated cells 24h after post infection (p.i.). Whereas the majority of non-

409   treated cells died 24h p.i., LiCl-treated cells grew to confluence displaying resistance to

410   infection (Fig. 5B).

411   Even though at higher MOI all cells died by 24 h p.i. regardless of LiCl treatment (Fig.

412   5A), at a MOI of 1 the percentage of cells detected as infected by fluorescent staining was

413   significantly lower at earlier times after infection (8h p.i.) among LiCl-treated cells than

414   among untreated cells (Fig. 5C and D). This is indicative of the capacity of LiCl-treated cells

415   to dampen the kinetics of virus multiplication.

416

417   **The canonical Wnt/β-catenin pathway is a major target of Rift Valley fever virus.**

418   Cellular pathways participating in the establishment of an effective antiviral response

419   are expected to be affected during viral infections: either "positively", leading to the

420   activation of the host antiviral response, or "negatively", in the case of viruses capable to

421   efficiently inhibit the cellular antiviral response. Therefore, if as suggested in this work, a

422   TCF/β-catenin transcription complex participates in the establishment of an efficient antiviral

423   response then pathways regulating active TCF/β-catenin complex formation are expected to

424   be targeted during viral infection.

425   The effect of a viral infection upon the canonical Wnt/β-catenin pathway, which is a

426   major regulator of the formation of active TCF/β-catenin complexes, was analyzed here

427   during infection with Rift Valley fever virus (RVFV) for which two different strains,

428   pathogenic and non-pathogenic are available. The wild type RVFV ZH548 strain (ZH) of the

429   virus that codes for a non-structural NSs protein, suppresses IFN-β expression and is highly

430   pathogenic causing severe illness in humans and animals (53-55), whereas the RVFV

431   ZH548ΔNSs strain (ΔNSs), deleted for the region coding for NSs protein, strongly activates

432   IFN-β expression and is fully avirulent (56).

433   The viral NSs protein, which is a major factor responsible of RVFV pathogenicity, has

434   the characteristic to form filamentous structures in nuclei of infected cells abnormally

435   trapping within these structures transcription factors and co-factors of the host (21,57).

436   During a recent genome wide search for regulatory DNA regions of the host interacting with

437   RVFV NSs protein, several genes associated with the canonical Wnt/β-catenin pathway were

438   identified as interacting with NSs (Table II) (58). Among these were genes coding for several

439   WNT ligands (*Wnt1*, *Wnt2*, *Wnt6* and *Wnt8b*), for antagonists of Wnt signaling (*Apcdd1*,

440   *Dkk1* and *Kremen2*), for members of the multiprotein complex regulating the degradation of

441   β-catenin (*Gsk3b*, *Gsk3a* and *Axin2*), for β-catenin itself (*Ctnnb1*) as well as for members of

442   the TCF/β-catenin complex (*Tcf7l2*, *Lef1* and *Bcl9*). Also, DNA regulatory sequences

443   associated with genes coding for casein kinases (*Csnk1d*, *Csnk1g2*, *Csnk1g3* and *Csnk2a2*)

444   known to positively regulate the canonical Wnt/β-catenin signaling pathway at different

445   levels were present among cellular DNA regions targeted by NSs.

446   Using RT-qPCR, we analyzed the effect of RVFV infection, either pathogenic (ZH

447   strain) or non-pathogenic (ΔNSs strain), upon the expression of the genes related to canonical

448   Wnt/β-catenin pathway identified as significantly interacting with NSs. For this, RNA was

449   purified from three different cell types targeted by RVFV (L929 fibroblasts, AML12

450   hepatocytes and bone marrow derived macrophages (BMDM)) either non-, ΔNSs- or ZH-

451   infected. After reverse transcription, the fold change in the expression level of genes of

452   interest (including the gene coding for IFN-β) was calculated with respect to non-infected

453   cells using three different reference genes (Fig. 6).

454   As expected, infection with the avirulent ΔNSs strain strongly activated IFN-β gene

455   expression in the three cell types tested, whereas infection with the virulent ZH strain

456   maintained the IFN-β expression in an abnormally repressed state.

457   Both strains affected the Wnt/β-catenin pathway but with opposite effects. Infection

458   with the non-pathogenic ΔNSs strain led to i) the activation of the expression of genes coding

459   for casein kinases, with *Csnk1d* and *Csnk2a2* genes activated in the three cell types tested,

460   and *Csnk1g3* activated in fibroblasts and BMDM; ii) the activation of the expression of genes

461   coding for factors essentials for the formation of an active β-catenin transcription complex

462   such as *Bcl9* and *Tcf7l2* in hepatocytes and BMDM; and iii) the repression of the expression

463   of the *Axin2* gene, a negative regulator of the canonical Wnt/β-catenin pathway (59), in

464   hepatocytes. On the contrary, infection with ZH led in BMDM to the inhibition of the

465   expression of *Csnk1d* and *Csnk2a2* genes, and the activation of the expression of *Axin2* gene.

466   Also, a slight inhibition of the expression of *Bcl9* gene was observed in fibroblasts and

467   hepatocytes.

468   As shown in Fig. 7, all the effects observed after non-pathogenic ΔNSs infection

469   tended towards the formation of an active nuclear β-catenin complex. On the contrary, the

470   effects observed after infection with the pathogenic ZH strain of the virus tended against the

471   formation of a nuclear β-catenin transcription complex.

472   Virus-induced IFN-β expression depends on the presence of several transcription

473   factors and co-factors that synergize to give rise to a maximum of expression (16-27).

474   Therefore, even though TCF/β-catenin complexes could participate on the induction of IFN-β

475   expression, they should not be considered as alone responsible of the strong IFNβ expression

476   induced during infection by ΔNSs. Similarly, even though RVFV targeting of TCF/β-catenin

477   complex formation could be participating in the RVFV-induced inhibition of IFN-β

478   expression, this should not be considered as alone responsible of the complete lack of IFN-β

479   expression in RVFV infected cells that we have previously shown to be related to the capacity

480   of NSs to maintain the IFN-β promoter region associated to a transcriptionally repressive

481   environment (16, 21).

482   Nevertheless, the fact that avirulent and virulent strains of RVFV had opposite, mirror,

483   effects upon the Wnt/β-catenin pathway suggested that this pathway could be playing a role in

484   mounting an efficient innate antiviral response against RVFV infection.

485

486   **A potential role for β-catenin protein in setting up an antiviral response against RVFV**

487   **infection.**

488   In order to test the effect of RVFV infection upon the level of β-catenin *in vivo*, the

489   presence of β-catenin was analyzed in the liver and brain of mice that were either non-

490   infected, or infected with ΔNSs or ZH strains. Of note, the liver and brain are two main

491   organs targeted during RVFV infection (60). Mice were euthanized at days 3 and 5 p.i. and

492   the liver and brain were removed; one half of each organ was used for total protein

493   purification and Western blot analysis and the other half for RNA purification and RT-qPCR

494   analysis. Whereas no variation was observed for β-catenin at the transcriptional level (data

495   not shown), Western blot analysis showed significant variations at the protein level in the

496   liver of ZH-infected mice at day 5 p.i. (Fig. 8A). Under these conditions, the average relative

497   level of β-catenin significantly diminished in the liver of all ZH-infected mice compared to

498   non-infected and ΔNSs-infected mice where on the contrary, the level of β-catenin was

499   increased in ΔNSs-infected mice (Fig. 8A).

500   Viral targeting of β-catenin was further analyzed with respect to the presence of the

501   virus (as translated by the presence of viral mRNAs coding for viral proteins N and NSs) in

502   the liver and the brain of each mouse under each condition. In the case of ZH-infected mice,

503   viral N and NSs mRNAs were clearly detected at day 5 p.i. in the liver of mouse #1, 2 and 3

504   and by day 3 p.i. in the liver of mouse #1 (Fig. 8B) but remained essentially undetectable in

505   the brain of infected mice. Therefore, the effect of RVFV infection upon the level of β-

506   catenin appeared correlated with the presence of the virus suggesting that β-catenin could be

507   playing a role protecting against ZH replication.

508   If as hypothesized β-catenin played a role in the antiviral response against RVFV

509   infection, then LiCl treatment should have a protective effect. In order to test this, L929 cells

510   were either non-treated or pretreated with LiCl during 24 h before infection with the virulent

511   ZH strain of RVFV. In agreement with a potential physiological role for β-catenin inhibiting

512   RVFV replication, pretreatment with LiCl significantly diminished the number of lytic

513   plaques induced by RVFV (Fig. 8C).

514

Discussion

515

516   In this work we have demonstrated that cell treatment with LiCl, an inhibitor of GSK-

517 3, leads to the enhancement of the constitutive (namely IRF3-NFκB-ATF2/cJUN-

518 independent) as well as virus-induced level of IFN-β gene expression, provided that LiCl

519 treatment be correlated with the IFN-β promoter recruitment of β-catenin. The effect of LiCl

520 on the constitutive as well as virus-induced transcriptional capacity of the IFN-β promoter

521 required the presence of the IFN-β promoter region containing TCF-binding sites, positioned

522 5' of the VRE region. Results obtained in this work with siRNA directed against β-catenin

523 added to results obtained with iCRT3, an inhibitor of TCF/β-catenin complexes (51) as well

524 as results obtained with IFN-β promoters carrying mutated TCF sites, demonstrated that the

525 capacity of LiCl to enhance IFN-β expression was mediated through TCF/β-catenin

526 complexes rather than IRF3 as suggested until now in the literature.

527   In the absence of β-catenin, TCFs act as transcriptional repressors recruiting co-

528 repressor complexes. The TCF sites we describe here on the IFNβ promoter are positioned

529 over the NRDII region that corresponds to a negative regulatory region. It is therefore

530 possible that in the absence of β-catenin, TCF factors could be participating in the

531 establishment of the repressive state of the IFN-β promoter alongside with other repressors

532 and co-repressors previously described as participating in the establishment of the repressive

533 state of the IFNβ promoter such as the SAP30/Sin3A/NCoR/HDAC3 complex (21).

534   Such capacity of LiCl to enhance the transcriptional activity of the IFN-β promoter,

535 we also observed it after treatment of the cells with SB216763 and inhibitor IX, which are

536 two other inhibitors of GSK-3, suggesting that the capacity of LiCl to enhance IFN-β

537 expression observed in this work could be the consequence of the inhibition of GSK-3 that is

538 a target that these three inhibitors have in common. In agreement with our results, activation

539   of IFN-β expression after GSK-3 inhibition by SB216763 has been previously described by

540   several groups in the context of the IFN-β expression induced in response to LPS or polyI:C

541   (39, 61, 62), and a positive effect for β-catenin on IFN-β expression has been reported under

542   different contexts (41, 43, 63).

543   However, inhibition of GSK-3 has also been associated to a negative effect on virus-

544   induced IFN-β expression (44). This was observed in the context of SeV infection and

545   required the SeV-induced secretion of WNT2B and WNT9 ligands that in association with the

546   nuclear accumulation of β-catenin triggered a negative feedback loop to reduce and control an

547   excessive IFN-β response. The SeV-dependent negative effect of GSK-3 inhibition on IFN-β

548   expression was shown to be independent of TCF/β-catenin driven transcription and therefore

549   different from the positive effect of GSK-3 inhibition we have observed here on IFN-β

550   expression. Even though the exact mechanism leading to IFN-β inhibition in the case of SeV

551   infection has remained undetermined, it was suggested to depend on the association of IRF3

552   with β-catenin, affecting the late stage of IRF3 transcriptional activity (44). In our study, the

553   TCF/β-catenin activation of IFN-β expression observed in the presence of LiCl, was observed

554   not only in non-infected cells but also after NDV infection including during the period of the

555   establishment of the post-transcriptional turn-off of the IFN-β gene (Fig. 1 I, 6 and 8 hr p.i.).

556   Differences between our results and those of Baril et al. could be related to the fact that

557   contrary to SeV, NDV infection does not induce WNT signaling as translated by the inability

558   of NDV to induce accumulation of nuclear β-catenin even at late times after infection.

559   WNT ligands lead to the nuclear accumulation of β-catenin through a mechanism

560   different from that of LiCl. While LiCl inhibits the kinase activity of GSK-3 preventing β-

561   catenin degradation, WNT ligands induce the plasma membrane recruitment of GSK-3 and

562   AXIN1, disrupting the cytoplasmic GSK3/AXIN/APC destruction complex of β-catenin.

563   Thus, WNT ligands lead to the accumulation of nuclear β-catenin without affecting the kinase

564   activity of GSK3. Lei et al. (64) have described a positive effect of GSK-3 upon IFN-β

565   expression and response independent of the kinase activity of GSK-3, that required the direct

566   interaction of GSK-3 with TBK1 necessary for the TBK1-dependent activation of IRF3 (64).

567   It is possible that the plasma membrane recruitment of GSK-3 induced by WNT ligands in the

568   context of SeV infection, could interfere with the capacity of GSK-3 to interact with and

569   activate TBK1, therefore diminishing through a feedback loop the pool of phosphorylated

570   active IRF3.

571   Our results showed that the LiCl-dependent activation of the IFN-β expression was

572   correlated with the induction of an effective antiviral response. This in agreement with

573   recently published data describing the capacity of LiCl to inhibit H7N7 influenza A (43) and

574   Porcine Reproductive and Respiratory Syndrome (PRRS) (65) virus replication. Interestingly,

575   both these works show results indicative of a role for TCF/β-catenin complexes on these

576   LiCl-dependent inhibitions of viral infection. Contrary to these and our results, Wang et al.

577   (62) have described a LiCl-dependent attenuation of IFN-β expression and viral infection,

578   through a mechanism independent of LiCl/β-catenin complexes related with the capacity of

579   LiCl to inhibition TBK1. To our knowledge, this is the only work that has described an

580   inhibitory effect of LiCl on TBK1. This is an effect of LiCl that we did not observe under our

581   experimental conditions. Notwithstanding that NDV-induced IFN-β expression relies on the

582   activation of RIG-I and TBK1, we never observed an inhibitory effect of LiCl treatment on

583   the IFN-β expression induced by NDV. Not even under conditions when the positive effect of

584   LiCl was not detected, such as when LiCl was unable to induce accumulation of nuclear β-

585   catenin in AML12 cells (Fig. 2 A-D) or unable to induce β-catenin recruitment as in the case

586   of the WT110 IFN-β promoter (Fig. 3). Differences between our results, as well as results

587   obtained in the context of influenza (43) and PPRS (65) virus, and the work of Wang et al.

588   (62) could result from variations on the state of TBK1 under our respective cellular models.

589   TBK1 is an enzyme whose activity strongly relies on its cellular localization that can be

590   affected by a wide diversity of mechanisms and signaling pathways including not only

591   pathogens but also cell growth and proliferation (66).

592   Further emphasizing the potential role for TCF/β-catenin complexes in the

593   establishment of an efficient innate antiviral response, we show here that LiCl treatment of

594   L929 cells protected these cells against the cytopathic effect of RVFV that we show here to

595   negatively target β-catenin in the liver of infected mice. Viral targeting of the formation of

596   active nuclear β-catenin transcription complexes has been observed in the context of

597   infections with other viruses such as influenza H1N1 virus, Human Cytomegalovirus

598   (HCMV), Venezuelan Equine Encephalitis Virus (VEEV) and HIV-1 (40,67-69). Such

599   tendency of viruses to negatively target β-catenin, is in a agreement with the scenario of a

600   positive role for β-catenin during the establishment of an efficient antiviral response.

601   Several reports in the literature point at physiological roles for constitutive IFN-β

602   expression in the absence of viral infection (33). However, little is known concerning the

603   mechanism(s) capable to directly modulate IFN-β expression in naïve cells except for results

604   obtained with *c-Jun*^{-/-} murine embryonic fibroblasts that identified transcription factor c-Jun

605   as a potential regulator of the constitutive level of IFN-β expression (70). Since inhibition of

606   GSK-3, leading to the formation of nuclear TCF/β-catenin complexes, can be reached not

607   only physiologically through pathways associated with Wnt ligands and Akt phosphorylation

608   but also pharmaceutically, results shown here open the possibility of a wide range of cellular

609   and extra-cellular mechanisms susceptible to modulate the level of IFN-β expression in the

610   absence of infection.

611   If we consider that TCF/β-catenin complexes can directly affect constitutive levels of

612   IFN-β expression in the absence of pathogens as described here, then the existence of cross-

613   talks between β-catenin and IFN-β should also be considered beyond the issue of pathogen

614   infection. For example, the capacity of β-catenin to modulate inflammatory and immune

615   responses (71) could be related to its ability to modulate the expression of IFN-β, which is a

616   major regulator of immunity and inflammatory responses. Also, a cross-talk between β-

617   catenin and IFN-β during the establishment and/or treatment of neurological disorders such as

618   Alzheimer disease and multiple sclerosis should be considered since both Wnt/β-catenin

619   pathway and IFN-β response have been associated to these neurological pathologies (72-74).

620   Although modulation of the constitutive level of IFN-β expression has probably been

621   observed in the past by many researchers, it has often been neglected because it seemed only

622   minor compared to pathogen-induced IFN-β expression. Nevertheless, even though weak, the

623   biological significance of constitutive IFN-β expression is no longer to be demonstrated (33).

624   Therefore, mechanisms capable to modulate constitutive IFN-β expression, such as the one

625   our results demonstrate here, should gain interest in the future.

626

627

628

629

630

631

632

633

634

635

636

637

646 **References**

647 1. **Stark GR, Kerr IM, Williams BR, Silverman RH, Schreiber RD.** 1998. How cells

648 respond to interferons. Annu Rev Biochem **67**:227-64.

649 2. **Stetson DB, Medzhitov R.** 2006. Type I interferons in host defense. Immunity **25**:373-81.

650 3. **Jensen S, Thomsen AR.** 2012. Sensing of RNA viruses: a review of innate immune

651 receptors involved in recognizing RNA virus invasion. J Virol **86**:2900-10

652 4. **Randall RE, Goodbourn S.** 2008. Interferons and viruses: an interplay between induction,

653 signalling, antiviral responses and virus countermeasures. J Gen Virol **89**:1-47.

654 5. **Deonarain R, Alcamí A, Alexiou M, Dallman MJ, Gewert DR, Porter AC.** 2000.

655 Impaired antiviral response and alpha/beta interferon induction in mice lacking beta

656 interferon. J Virol **74**:3404-9.

657 6. **Müller U, Steinhoff U, Reis LF, Hemmi S, Pavlovic J, Zinkernagel RM, Aguet M.**

658 1994. Functional role of type I and type II interferons in antiviral defense. Science **264**:1918-

659 21.

660 7. **Hwang SY, Hertzog PJ, Holland KA, Sumarsono SH, Tymms MJ, Hamilton JA,**

661 **Whitty G, Bertoncello I, Kola I.** 1995. A null mutation in the gene encoding a type I

662 interferon receptor component eliminates antiproliferative and antiviral responses to

663 interferons alpha and beta and alters macrophage responses. Proc Natl Acad Sci USA

664 **92**:11284-8.

665 8. **Hall JC, Rosen A.** 2010. Type I interferons: crucial participants in disease amplification in

666 autoimmunity. Nat. Rev. Rheumatol. **6**:40-9.

667 9. **Crow MK.** 2010. Type I interferon in organ-targeted autoimmune and inflammatory

668 diseases. Arthritis Res Ther **12**(Suppl 1):S5.

669 10. **Choubey D, Moudgil KD.** 2011. Interferons in autoimmune and inflammatory diseases:

670 regulation and roles. J Interferon Cytokine Res **31**:857-65.

671 11. **Trinchieri G.** 2010. Type I interferon: friend or foe? J Exp Med **207**:2053-63.

672 12. **Prinz M, Knobeloch KP.** 2012. Type I interferons as ambiguous modulators of chronic

673 inflammation in the central nervous system. Front Immunol **3**:67.

674 13. **Hu J, Sealfon SC, Hayot F, Jayaprakash C, Kumar M, Pendleton AC, Ganee A,**

675 **Fernandez-Sesma A, Moran TM, Wetmur JG.** 2007. Chromosome-specific and noisy

676 IFNB1 transcription in individual virus-infected human primary dendritic cells. Nucleic Acids

677 Res **35**:5232-41.

678 14. **Zhao M, Zhang J, Phatnani H, Scheu S, Maniatis T.** 2012. Stochastic expression of the

679 interferon-β gene. PLoS Biol **10**:e1001249.

680 15. **Apostolou E, Thanos D.** 2008. Virus Infection Induces NF-kappaB-dependent

681 interchromosomal associations mediating monoallelic IFN-beta gene expression. Cell **134**:85-

682 96.

683 16. **Josse T, Mokrani-Benhelli H, Benferhat R, Shestakova E, Mansuroglu Z,**

684 **Kakanakou H, Billecocq A, Bouloy M, Bonnefoy E.** 2012. Association of the interferon-β

685 gene with pericentromeric heterochromatin is dynamically regulated during virus infection

686 through a YY1-dependent mechanism. Nucleic Acids Res **40**:4396-411.

687 17. **Maniatis T, Falvo JV, Kim TH, Kim TK, Lin CH, Parekh BS, Wathelet MG.** 1998.

688 Structure and function of the interferon-beta enhanceosome. Cold Spring Harb Symp Quant

689 Biol **63**:609-20.

690 18. **Agalioti T, Lomvardas S, Parekh B, Yie J, Maniatis T, Thanos D.** 2000. Ordered

691 recruitment of chromatin modifying and general transcription factors to the IFN-beta

692 promoter. Cell **103**:667-78.

693   19. **Agalioti T, Chen G, Thanos D.** 2002. Deciphering the transcriptional histone acetylation

694   code for a human gene. Cell **111**:381-92.

695   20. **Mokrani H, Sharaf el Dein O, Mansuroglu Z, Bonnefoy E.** 2006. Binding of YY1 to

696   the proximal region of the murine beta interferon promoter is essential to allow CBP

697   recruitment and K8H4/K14H3 acetylation on the promoter region after virus infection. Mol

698   Cell Biol **26**:8551-61.

699   21. **Le May N, Mansuroglu Z, Léger P, Josse T, Blot G, Billecocq A, Flick R, Jacob Y,**

700   **Bonnefoy E, Bouloy M.** 2008. A SAP30 complex inhibits IFN-beta expression in Rift Valley

701   fever virus infected cells. PLoS Pathog **4**:e13.

702   22. **Sato M, Taniguchi T, Tanaka N.** 2001. The interferon system and interferon regulatory

703   factor transcription factors -- studies from gene knockout mice. Cytokine Growth Factor Rev

704   **12**:133-42.

705   23. **Kim TK, Kim TH, Maniatis T.** 1998. Efficient recruitment of TFIIB and CBP-RNA

706   polymerase II holoenzyme by an interferon-beta enhanceosome in vitro. Proc Natl Acad Sci U

707   S A **95**:12191-6.

708   24. **Panne D, Maniatis T, Harrison SC.** 2004. Crystal structure of ATF-2/c-Jun and IRF-3

709   bound to the interferon-beta enhancer. EMBO J **23**:4384-93.

710   25. **Klar M, Bode J.** 2005. Enhanceosome formation over the beta interferon promoter

711   underlies a remote-control mechanism mediated by YY1 and YY2. Mol Cell Biol **25**:10159-

712   70.

713   26. **Siednienko J, Maratha A, Yang S, Mitkiewicz M, Miggin SM, Moynagh PN.** 2011.

714   Nuclear factor κB subunits RelB and cRel negatively regulate Toll-like receptor 3-mediated

715   β-interferon production via induction of transcriptional repressor protein YY1. J Biol Chem

716   **286**:44750-63.

717   27. **Weill L, Shestakova E, Bonnefoy E.** 2003. Transcription factor YY1 binds to the murine

718   beta interferon promoter and regulates its transcriptional capacity with a dual

719   activator/repressor role. J Virol **77**:2903-14.

720   28. **Dafny N, Yang PB.** 2005. Interferon and the central nervous system. Eur J Pharmacol

721   **523**:1-15.

722   29. **Prinz M, Schmidt H, Mildner A, Knobeloch KP, Hanisch UK, Raasch J, Merkler D,**

723   **Detje C, Gutcher I, Mages J, Lang R, Martin R, Gold R, Becher B, Brück W, Kalinke U.**

724   2008. Distinct and nonredundant in vivo functions of IFNAR on myeloid cells limit

725   autoimmunity in the central nervous system. Immunity **28**:675-86.

726   30. **Hata N, Sato M, Takaoka A, Asagiri M, Tanaka N, Taniguchi T.** 2001. Constitutive

727   IFN-alpha/beta signal for efficient IFN-alpha/beta gene induction by virus. Biochem Biophys

728   Res Commun **285**:518-25.

729   31. **Haller O, Arnheiter H, Gresser I, Lindenmann J.** 1979. Genetically determined,

730   interferon-dependent resistance to influenza virus in mice. J Exp Med **149**:601-12.

731   32. **Vogel SN, Fertsch D.** 1984. Endogenous interferon production by endotoxin-responsive

732   macrophages provides an autostimulatory differentiation signal. Infect Immun **45**:417-23.

733   33. **Gough DJ, Messina NL, Clarke CJ, Johnstone RW, Levy DE.** 2012. Constitutive type

734   I interferon modulates homeostatic balance through tonic signaling. Immunity **36**:166-74.

735   34. **MacDonald BT, Tamai K, He X.** 2009. Wnt/beta-catenin signaling: components,

736   mechanisms, and diseases. Dev Cell **17**:9-26.

737   35. **Valenta T, Hausmann G, Basler K.** 2012. The many faces and functions of β-catenin.

738   EMBO J **31**:2714-36.

739   36. **Sampietro J, Dahlberg CL, Cho US, Hinds TR, Kimelman D, Xu W.** 2006. Crystal

740   structure of a beta-catenin/BCL9/Tcf4 complex. Mol Cell **24**:293-300.

741   37. **Deka J, Wiedemann N, Anderle P, Murphy-Seiler F, Bultinck J, Eyckerman S,**

742   **Stehle JC, André S, Vilain N, Zilian O, Robine S, Delorenzi M, Basler K, Aguet M.** 2010.

743   Bcl9/Bcl9l are critical for Wnt-mediated regulation of stem cell traits in colon epithelium and

744   adenocarcinomas. Cancer Res **70**:6619-28.

745   38. **Archbold HC, Yang YX, Chen L, Cadigan KM.** 2011. How do they do Wnt they do?:

746   regulation of transcription by the Wnt/β-catenin pathway. Acta Physiol (Oxf) **204**:74-109.

747   39. **Wang H, Garcia CA, Rehani K, Cekic C, Alard P, Kinane DF, Mitchell T, Martin M.**

748   2008. IFN-beta production by TLR4-stimulated innate immune cells is negatively regulated

749   by GSK3-beta. J Immunol **181**:6797-802.

750   40. **Shapira SD, Gat-Viks I, Shum BO, Dricot A, de Grace MM, Wu L, Gupta PB, Hao**

751   **T, Silver SJ, Root DE, Hill DE, Regev A, Hacohen N.** 2009. A physical and regulatory map

752   of host-influenza interactions reveals pathways in H1N1 infection. Cell **139**:1255-67.

753   41. **Yang P, An H, Liu X, Wen M, Zheng Y, Rui Y, Cao X.** 2010. The cytosolic nucleic

754   acid sensor LRRFIP1 mediates the production of type I interferon via a beta-catenin-

755   dependent pathway. Nat Immunol **11**:487-94.

756   42. **Zhu J, Coyne CB, Sarkar SN.** 2011. PKC alpha regulates Sendai virus-mediated

757   interferon induction through HDAC6 and β-catenin. EMBO J **30**:4838-49.

758   43. **Hillesheim A, Nordhoff C, Boergeling Y, Ludwig S, Wixler V.** 2014. β-catenin

759   promotes the type I IFN synthesis and the IFN-dependent signaling response but is suppressed

760   by influenza A virus-induced RIG-I/NF-κB signaling. Cell Commun Signal **12**:29.

761   44. **Baril M, Es-Saad S, Chatel-Chaix L, Fink K, Pham T, Raymond VA, Audette K,**

762   **Guenier AS, Duchaine J, Servant M, Bilodeau M, Cohen E, Grandvaux N, Lamarre D.**

763   2013. Genome-wide RNAi screen reveals a new role of a WNT/CTNNB1 signaling pathway

764   as negative regulator of virus-induced innate immune responses. PLoS Pathog **9**:e1003416.

765 45. **Bonnefoy E, Bandu MT, Doly J.** 1999. Specific binding of high-mobility-group I

766 (HMGI) protein and histone H1 to the upstream AT-rich region of the murine beta interferon

767 promoter: HMGI protein acts as a potential antirepressor of the promoter. Mol Cell Biol

768 **19**:2803-16.

769 46. **Gommet C, Billecocq A, Jouvion G, Hasan M, Zaverucha do Valle T, Guillemot L,**

770 **Blanchet C, van Rooijen N, Montagutelli X, Bouloy M, Panthier JJ.** 2011. Tissue tropism

771 and target cells of NSs-deleted rift valley fever virus in live immunodeficient mice. PLoS

772 Negl Trop Dis **5**:e1421.

773 47. **Yadani FZ, Kohl A, Préhaud C, Billecocq A, Bouloy M.** 1999. The carboxy-terminal

774 acidic domain of Rift Valley Fever virus NSs protein is essential for the formation of

775 filamentous structures but not for the nuclear localization of the protein. J Virol **73**:5018-25.

776 48. **Taniguchi T, Takaoka A.** 2001. A weak signal for strong responses: interferon-

777 alpha/beta revisited. Nat Rev Mol Cell Biol **2**:378-86.

778 49. **Solomon MJ, Strauss F, Varshavsky A.** 1986. A mammalian high mobility group

779 protein recognizes any stretch of six A.T base pairs in duplex DNA. Proc Natl Acad Sci USA

780 **83**:1276-80.

781 50. **van de Wetering M, Clevers H.** 1992. Sequence-specific interaction of the HMG box

782 proteins TCF-1 and SRY occurs within the minor groove of a Watson-Crick double helix.

783 EMBO J **8**:3039-44.

784 51. **Gonsalves FC, Klein K, Carson BB, Katz S, Ekas LA, Evans S, Nagourney R,**

785 **Cardozo T, Brown AM, DasGupta R.** 2011. An RNAi-based chemical screen identifies

786 three small-molecule inhibitors of the Wnt/*wingless* signaling pathway. Proc Natl Acad Sci

787 USA **108**:5954-63.

788 52. **Shestakova E, Bandu MT, Doly J, Bonnefoy E.** 2001. Inhibition of histone

789 deacetylation induces constitutive derepression of the beta interferon promoter and confers

790 antiviral activity. J Virol **75**:3444-52.

791 53. **Pepin M, Bouloy M, Bird BH, Kemp A, Paweska J.** 2010. Rift Valley fever

792 virus(Bunyaviridae: Phlebovirus): an update on pathogenesis, molecular epidemiology,

793 vectors, diagnostics and prevention. Vet Res **6**:61.

794 54. **do Valle TZ, Billecocq A, Guillemot L, Alberts R, Gommet C, Geffers R, Calabrese**

795 **K, Schughart K, Bouloy M, Montagutelli X, Panthier JJ.** 2010. A new mouse model

796 reveals a critical role for host innate immunity in resistance to Rift Valley fever. J Immunol

797 **185**:6146-56.

798 55. **Ikegami T.** 2012. Molecular biology and genetic diversity of Rift Valley fever virus.

799 Antiviral Res. **95**:293-310.

800 56. **Billecocq A, Gauliard N, Le May N, Elliott RM, Flick R, Bouloy M.** 2008. RNA

801 polymerase I-mediated expression of viral RNA for the rescue of infectious virulent and

802 avirulent Rift Valley fever viruses. Virology **378**:377-84.

803 57. **Le May N, Dubaele S, Proietti De Santis L, Billecocq A, Bouloy M, Egly JM.** 2004.

804 TFIIH transcription factor, a target for the Rift Valley hemorrhagic fever virus. Cell **116**:541-

805 50.

806 58. **Benferhat R, Josse T, Albaud B, Gentien D, Mansuroglu Z, Marcato V, Souès S, Le**

807 **Bonniec B, Bouloy M, Bonnefoy E.** 2012. Large-scale chromatin immunoprecipitation with

808 promoter sequence microarray analysis of the interaction of the NSs protein of Rift Valley

809 fever virus with regulatory DNA regions of the host genome. J Virol **86**:11333-44.

810 59. **Jho EH, Zhang T, Domon C, Joo CK, Freund JN, Costantini F.** 2002. Wnt/beta-

811 catenin/Tcf signaling induces the transcription of Axin2, a negative regulator of the signaling

812 pathway. Mol Cell Biol **22**:1172-83.

813 60. **Reed C, Steele KE, Honko A, Shamblin J, Hensley LE, Smith DR.** 2012.

814 Ultrastructural study of Rift Valley fever virus in the mouse model. Virology **431**:58-70.

815 61. **Gantner BN, Jin H, Qian F, Hay N, He B, Ye RD.** 2012. The Akt1 isoform is required

816 for optimal IFN-β transcription through direct phosphorylation of β-catenin. J Immunol

817 **189**:3104-11.

818 62. **Wang L, Zhang L, Zhao X, Zhang M, Zhao W, Gao C.** 2013. Lithium attenuates IFN-

819 β production and antiviral response via inhibition of TANK-Binding Kinase 1 kinase activity.

820 J Immunol **191**:4392-8.

821 63. **Ma F, Liu SY, Razani B, Arora N, Li B, Kagechika H, Tontonoz P, Núñez V, Ricote**

822 **M, Cheng G.** 2014. Retinoid X receptor α attenuates host antiviral response by suppressing

823 type I interferon. Nat Commun **5**:5494.

824 64. **Lei CQ, Zhong B, Zhang Y, Zhang J, Wang S, Shu HB.** 2010. Glycogen synthase

825 kinase 3β regulates IRF3 transcription factor-mediated antiviral response via activation of the

826 kinase TBK1. Immunity **33**:878-89.

827 65. **Hao HP, Wen LB, Li JR, Wang Y, Ni B, Wang R, Wang X, Sun MX, Fan HJ, Mao**

828 **X.** 2015. LiCl inhibits PRRSV infection by enhancing Wnt/β-catenin pathway and

829 suppressing inflammatory responses. Antiviral Res 117 :99-109.

830 66. **Helgason E, Phung QT, Dueber EC.** 2013. Recent insights into the complexity of Tank-

831 binding kinase 1 signaling networks: the emerging role of cellular localization in the

832 activation and substrate specificity of TBK1. FEBS Lett **587**:1230-7.

833 67. **Angelova M, Zwezdaryk K, Ferris M, Shan B, Morris CA, Sullivan DE.** 2012. Human

834 cytomegalovirus infection dysregulates the canonical Wnt/β-catenin signaling pathway. PLoS

835 Pathog **8**:e1002959.

836 68. **Kehn-Hall K, Narayanan A, Lundberg L, Sampey G, Pinkham C, Guendel I, Van**

837 **Duyne R, Senina S, Schultz KL, Stavale E, Aman MJ, Bailey C, Kashanchi F.** 2012.

838   Modulation of GSK-3β activity in Venezuelan equine encephalitis virus infection. PLoS One

839   **7**:e34761.

840   69. **Henderson LJ, Sharma A, Monaco MC, Major EO, Al-Harthi L.** 2012. Human

841   immunodeficiency virus type 1 (HIV-1) transactivator of transcription through its intact core

842   and cysteine-rich domains inhibits Wnt/β-catenin signaling in astrocytes: relevance to HIV

843   neuropathogenesis. J Neurosci **32**:16306-13.

844   70. **Gough DJ, Messina NL, Hii L, Gould JA, Sabapathy K, Robertson AP, Trapani JA,**

845   **Levy DE, Hertzog PJ, Clarke CJ, Johnstone RW.** 2010. Functional crosstalk between type

846   I and II interferon through the regulated expression of STAT1. PLoS Biol **8**:e1000361.

847   71**. Manicassamy S, Reizis B, Ravindran R, Nakaya H, Salazar-Gonzalez RM, Wang**

848   **YC, Pulendran B.** 2010. Activation of beta-catenin in dendritic cells regulates immunity

849   versus tolerance in the intestine. Science **329**:849-53.

850   72. **Taylor JM, Minter MR, Newman AG, Zhang M, Adlard PA, Crack PJ.** 2013. Type-1

851   interferon signaling mediates neuro-inflammatory events in models of Alzheimer's disease.

852   Neurobiol. Aging **35**:1012-23.

853   73. **Xie C, Li Z, Zhang GX, Guan Y.** 2013. Wnt Signaling in Remyelination in Multiple

854   Sclerosis: Friend or Foe? Mol Neurobiol **49**:1117-25.

855   74. **Rosso SB, Inestrosa NC.** 2013. WNT signaling in neuronal maturation and

856   synaptogenesis. Front Cell Neurosci **7**:103.

857

Figure legends

859 **Figure 1. LiCl treatment enhances the constitutive and virus-induced IFN-β expression.**

860 **(A)** Schematic representation of the general organization of the murine IFN-β promoter

861 showing the Negative Regulatory Domain (NRD) I and II as well as the Virus Responsive

862 Element (VRE). (**B** and **H**) Immunolocalisation of β-catenin in L929. Cells were either non-

863 treated (NT), treated with 20mM LiCl (LiCl) during 24h, or infected with NDV, labeled with

864 an anti-β-catenin antibody (a, d, g, h) and a DNA intercalating agent to visualize the nucleus

865 (ToPro3; b, e, h, k). Nuclei were outlined as shown in merge images and total green pixel

866 intensity corresponding to β-catenin labeling in the nucleus was quantified **(C).** β-catenin was

867 analyzed by Western blot (**D**) in nuclear extracts from L929 cells either non treated (NT) or

868 treated with 20 mM LiCl (LiCl) during 24h. IFN-β mRNA (**E** and **I**) and Oas1b or IRF7

869 mRNA (**F**) were analyzed by RT-qPCR: in non-infected L929 cells either non-treated (NT) or

870 LiCl treated (LiCl) (**E-G**); at different times post-infection (p.i) in L929 cells mock- or NDV-

871 infected, either non-treated (NT) or pre-treated with LiCl (LiCl) (**I**). In (**E-G**), the

872 corresponding fold inductions were calculated with respect to non treated cells; and in (**I**), the

873 corresponding fold inductions were calculated with respect to non-infected and non-treated

874 cells. **C**) n=33 (minimum) to 71 (maximum) counted nuclei; **E**) n=42 from 13 independent

875 experiences; **F**) n=18 from 6 independent experiences; **I**) n=6. Student test: p-value less than

876 0.001 (***), 0.01 (**) and 0.05 (*). All images correspond to one confocal section. Scale bar

877 = 10μM.

878

879 **Figure 2. LiCl enhancement of IFN-β expression is mediated by β-catenin. (A-D)** AML12

880 cells were either non-treated (NT) or treated with 20mM LiCl (LiCl) during 24h and either

881 non-infected (**A-C**) or NDV-infected (**D**). (**A** and **B**) Cells were labeled with an anti-β-catenin

882 antibody (a, d) and a DNA intercalating agent to visualize the nucleus (ToPro3; b, e). Nuclei

883   were outlined as shown in merge images (c, f), and total green pixel intensity corresponding

884   to β-catenin labeling in the nucleus was quantified (**B**). IFN-β mRNA (**C** and **D**) was

885   analyzed by RT-qPCR in non-infected (**C**) and NDV-infected (6h p.i.) (**D**) cells either non-

886   treated (NT) or pre-treated with LiCl (LiCl). The corresponding fold inductions were

887   calculated with respect to non-treated (**C**) or non-infected and non-treated (**D**) cells. (**E-G**)

888   L929 cells were either mock-transfected (mock) or transfected with β-catenin specific (siβcat)

889   or control (siCtrl) siRNA for 72h. β-catenin mRNA (**E**) and protein level (**F**) were analyzed

890   by RT-qPCR and WB respectively. (**G**) Post-siRNA, cells were either non-treated (NT) or

891   treated with 20mM LiCl (LiCl) during 24h before being NDV-infected. IFN-β mRNA was

892   analyzed by RT-qPCR. (**E** and **G**) the corresponding fold inductions were calculated with

893   respect to mock-transfected, non-treated and NDV-infected cells (n=3). Student test: p-value

894   less than 0.001 (***) and 0.01 (**). All images correspond to one confocal section. Scale bar

895   = 10μM.

896   **Figure 3. Interaction of β-catenin with the IFN-β promoter region containing a TCF**

897   **binding site is necessary for LiCl enhancement of IFN-β promoter activity. (A)**

898   Schematic representation of the WT330 and WT110 murine IFN-β promoters fused to the

899   CAT reporter gene and integrated into the genome of L929 WT330 and L929 WT110 cell

900   lines respectively. **(B to D)** β-catenin binding to WT330 and WT110 promoters and

901   corresponding CAT activities were analysed in L929 WT330 and WT110 cells either non-

902   treated (NT) or treated with LiCl 20mM (LiCl). **(B)** Genomic DNA was collected 24h post-

903   LiCl treatment and immunoprecipited with anti β-catenin (α-β-cat) or anti NSs (α-NSs,

904   negative control) antibodies. Increasing amounts (μL) of immunuprecipitated DNA (IP), as

905   well as non immunoprecipitated genomic DNA (Input) were amplified by semi-quantitative

906   PCR using specific primers for the WT330 and WT110 integrated promoters. **(C)** Cells were

907 collected post-LiCl treatment and their CAT activities quantified. The corresponding fold

908 inductions were calculated with respect to non-treated cells (n=12 for WT330 and n=6 for

909 WT110 cell lines). (**D**) Post-LiCl treatment, cells were further mock- or NDV-infected,

910 collected at different times post-infection and the corresponding CAT activities were

911 quantified. The corresponding fold inductions were calculated with respect to non-infected

912 non-treated cells (n=4). (**E and F**) CAT activities of L929 cells either non-treated (NT) or

913 treated with 50 µM of SB216763 (**E**) or 30µM of IX inhibitor during 24h (**F**). Cells were

914 further mock- or NDV-infected, collected 8h post-infection and the corresponding CAT

915 activities quantified. The corresponding fold inductions were calculated with respect to non-

916 infected non-treated cells.

917

918 **Figure 4. TCF binding sites mediate LiCl-dependent activation of the IFN-β promoter.**

919 (**A** and **B**) Equal amounts of nuclear extracts (N.E) prepared from L929 either non-treated (-

920 LiCl) or treated with 20mM LiCl (+LiCl) during 24h were incubated with the radioactively

921 labeled probes corresponding to wild type TCFa (TCFA) and TCFb (TCFB) or mutated TCFa

922 (TCFmutA) and TCFb (TCFmutB) sites. When indicated, nuclear extracts were incubated

923 with 500 ng of poly dI/dC or anti-β-catenin antibodies before adding the probes. (**C**) L929

924 cells transfected with plasmids containing luciferase reporter gene under the control of the

925 IFN-β promoter either WT or mutated at the TCFa site (mutA), the TCFb site (mutB) or the

926 TCFa and b sites (mutAB) were either non-treated (NT) or pre-treated with LiCl (LiCl) before

927 infection with NDV. Cells were collected 7h p.i. and the luminescence was quantified with

928 n=3. (**D** and **E**) L929 cells were either non-treated (NT) or treated with 20mM LiCl (LiCl)

929 during 24h or 48h in the presence or absence of iCRT3 before being NDV-infected. IFN-β

930 (**D**) or cyclin D1 (**E**) mRNA was analyzed by RT-qPCR and the corresponding fold

931   inductions were calculated with respect to non-treated NDV-infected (**D**) or non-infected (**E**)

932   cells; **D**) n=3. Student test: p-value less than 0.01 (******) and 0.05 (*****).

933   **Figure 5. LiCl treatment confers an antiviral state.** Monolayers of L929 cells either non-

934   treated (NT) or pre-treated with LiCl 20mM for 24h were infected with VSV. (**A**) Cytopathic

935   effect induced by increasing MOI of VSV was assayed by crystal violet dye staining 24h after

936   infection; (**B**) Photographs of typical culture fields. (**C** and **D**) Cells were fixed 8h after

937   infection (MOI=1), labeled with an antibody directed against the N protein of VSV (displayed

938   in gray) and ToPro3 (blue); merge images of the corresponding culture fields are displayed in

939   (**C**). The % of infected cells, as determined by the presence of N protein encoded by VSV

940   (fluorescence displayed in gray) was determined from a total of 7876 untreated and 9024

941   LiCl-treated cells counted with n=4 (**D**).

942

943   **Figure 6. Infection with RVFV affects the Wnt/β-catenin pathway at the transcriptional**

944   **level.** The expression of genes associated to the Wnt/β-catenin pathway previously identified

945   as interacting with the NSs protein of RVFV (listed in Table II) was measured in three

946   different cell types corresponding to fibroblast (L929), hepatocytes (AML12) and Bone

947   Marrow Derived Macrophages (BMDM) either mock-, RVFZH548- (ZH) or RVFVΔNSs-

948   (ΔNSs) infected. RNAs purified from mock- or virus-infected cells (8h p.i.) were analyzed by

949   RT-qPCR with primers specific for each gene of interest. The change in gene expression was

950   calculated in ZH and ΔNSs-infected cells with respect to mock-infected cells. The horizontal

951   broken lines indicate the cutoff value for upregulation (+1.5 fold) and downregulation (-1.5

952   fold). The effect of virus infection upon the expression of genes coding for WNT ligands as

953   well as for antagonist of Wnt signaling (*Apcdd1*, *Dkk1* and *Kremen2*) could not be tested

954   since the corresponding mRNA remained undetectable in the three cell types analyzed here.

955   n≥3 for each cell line.

956

Figure 7. Non-pathogenic and pathogenic strains of RVFV have opposite effects on the Wnt/β-catenin pathway. Genes participating in the Wnt/β-catenin pathway whose promoter regions were identified as significantly interacting with RVFV NSs protein during ChIP-on-chip experiments, listed in Table II, are shown in gray. Genes whose expressions were affected after infection with either the non-pathogenic ΔNSs or the pathogenic ZH strain of RVFV with respect to mock-infected cells are indicated by blue (upregulated) or red (downregulated) arrows.

964

Figure 8. A physiological relevance for β-catenin protein level during RVFV infection. **(A** and **B)** β-catenin protein and viral N and NSs RNA levels were evaluated in liver and brain of mice either non-infected (NI) or at days 3 and 5 p.i. with RVFVZH548 (ZH) or RVFVΔNSs (ΔNSs). **(A)** β-catenin protein level was analysed by Western blot and estimated densitometrically by comparison with the band intensity of GAPDH; values were averaged from (n) independent samples per time point with n=3 mice (NI), n=6 mice (ZH 3 days and ΔNSs 3 and 5 days) and n=4 mice (ZH 5 days). Fold induction was calculated by comparison of the relative β-catenin level in infected versus non-infected (NI) samples. **(B)** The relative level of viral N and NSs mRNA were estimated by comparison with the expression of three reference genes (Ppib, Hprt1 and Utp6c). **(C)** Number of lytic plaques formed in monolayers of L929 cells either non treated or pre-treated with LiCl 20 mM during 24h and infected with RVFVZH548. Cells were fixed and stained with crystal violet 3 days p.i. (n=4). Student test: p-value less than 0.001 (***), 0.01 (**) and 0.05 (*). All images correspond to one confocal section.

979

Table I. Sequences of the different primers used during qPCR assays.

	Forward	Reverse
Ppib	GGAGATGGCACAGGAGGAAA	CCGTAGTGCTTCAGTTTGAAGTTCT
Hprt1	TCCTCCTCAGACCGCTTTT	CCTGGTTCATCATCGCTAATC
Utp6c	TTTCGGTTGAGTTTTTCAGGA	CCCTCAGGTTTACCATCTTGC
Rplp0	CACTGGTCTAGGACCCGAGAAG	GGTGCCTCTGGAGATTTTCG
Ifnb1	ATGAACAACAGGTGGATCCTCC	AGGAGCTCCTGACATTTCCGAA
Os1b	GAGGTGCCGACGGAGGT	TCCAGATGAAGTCTTCCCAAAG
IRF7	CAGCGAGTGCTGTTTGGAGAC	AAGTTCGTACACCTTATGCGG
Ctnnb1	GCCACAGGATTACAAGAAGC	CCACCAGAGTGAAAAGAACG
Bcl9	AGTGCTCTCTCCAGGATATGATG	GGGCAAAGAGTGTGAAATGTTG
Csnk1d	ACGCCGGGATCGAGAAGAA	CCGACCGGGAATCTGTGAG
Csnk1g2	CAAACTTCCGAGTCGGCAAGA	GCTTGTAAAAGCGGTACTCCAG
Csnk1g3	TGGGACCGAGTTTGGAGGATT	CTGGCCGTCCTATTAAGAAGTTC
Csnk2a2	TCCCGAGCTGGGGTAATCAA	TGTTCCACCACGAAGGTTCTC
Tcf7l2	CACGACAGGAGGATTCAGA	GGGGCTTCTTCTTCTCTTC
Axin2	TGACTCTCCTTCCAGATCCCA	TGCCCACACTAGGCTGACA
Gsk3b	TGGCAGCAAGGTAACCACAG	CGGTTCTTAAATCGCTTGTCCTG

981

982 **Table II.** List of canonical Wnt/β-catenin genes whose regulatory DNA regions were
983 identified as interacting with RVFV NSs protein during ChIP-on-chip assays (55).

| Gene	Chromo-some	NSs interacting Region Start	Region Length (bps)	Probes in Region	p-value
Apcdd1	Chr18	63078268	563	16	0.007658
Axin2	Chr11	108827835	502	14	0.00618531
Bcl9	Chr3	97004948	751	21	0.00823024
Csnk1d	Chr11	120859171	651	18	0.0033914
Csnk1g2	Chr10	80096623	865	24	0.00136329
Csnk1g2	Chr10	80082196	920	22	0.00671548
Csnk1g3	Chr18	54109583	850	18	0.00104351
Csnk1g3	Chr18	54156237	499	10	0.00828074
Csnk2a2	Chr8	97965333	511	12	0.00827232
Ctnnb1	Chr9	120803511	517	15	0.00766641
Gsk3a	Chr7	26016588	488	14	0.00998065
Gsk3b	Chr16	38213326	554	16	0.006564
Kremen2	Chr17	23882003	542	14	0.00559623
Lef1	Chr3	130837713	488	13	0.00916435
Tcf7l2	Chr19	55894582	531	15	0.00931583
Wnt1	Chr15	98620114	407	11	0.00822183
Wnt2	Chr6	17981380	579	17	0.00595809
Wnt6	Chr1	74823318	824	23	0.00226374
Wnt6	Chr1	74830849	550	14	0.00750652
Wnt6	Chr1	74828942	494	14	0.00782631
Wnt6	Chr1	74818891	394	11	0.00812085
Wnt6	Chr1	74816494	489	13	0.00885298
Wnt8b	Chr19	44545480	754	20	0.00226374
Wnt8b	Chr19	44544618	808	23	0.00506606
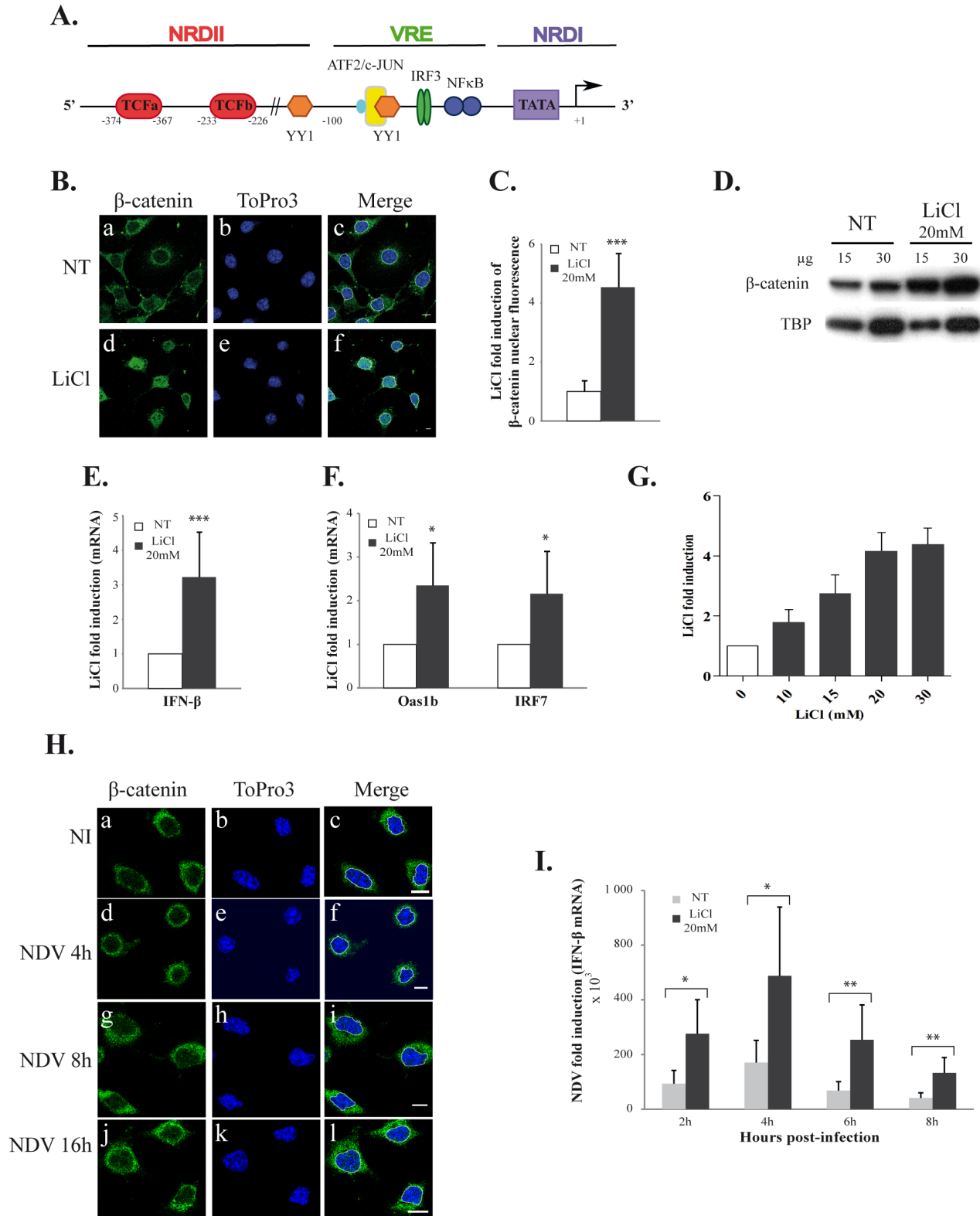
Figure 1. **LiCl treatement enhances the constitutive and virus-induced IFN-β expression**. (**A**) Schematic representation of the general organization of the murine IFN-β promoter showing the Negative Regulatory Domain (NRD) I and II as well as the Virus Responsive Element (VRE). (**B** and **H**) Immunolocalisation of β-catenin in L929 cells. Cells were either non-treated (NT), treated with 20mM LiCl (LiCl) during 24h, non infected (NI) or infected with NDV, labeled with an anti-β-catenin antibody (a,d,g,j) and a DNA intercalating agent to visualize the nucleus (ToPro3; b,e,h,k). Nuclei were outlined as shown in merge images, and total green pixel intensity corresponding to β-catenin labeling in the nucleus was quantified (**C**) . β-catenin protein level was analyzed by Western Blot (**D**) in nuclear extracts from L929 cells either non treated (NT) or treated with 20mM LiCl (LiCl) during 24h. IFN-β mRNA (**E** and **I**) and Oas1b or IRF7 mRNA (**F**) were analyzed by RT-qPCR: in non-infected L929 cells either non-treated (NT) or LiCl treated (LiCl) (**E - G**); at different times post-infection (p.i) in L929 cells mock- or NDV-infected, either non-treated (NT) or pre-treated with LiCl (LiCl) (**I**). In (**E - G**), the corresponding fold inductions were calculated with respect to non-treated cells; and in (**I**), the corresponding fold inductions were calculated with respect to non-infected and non-treated cells. **C**) n=33 (minimum) to 71 (maximum) counted nuclei; **E**) n=42 from 13 independent experiences; **F**) n=18 from 6 independent experiences; **I**) n=6. Student test: p-value less than 0.001 (***), 0.01 (**) and 0.05 (*). All images correspond to one confocal section. Scale bar = 10μM.
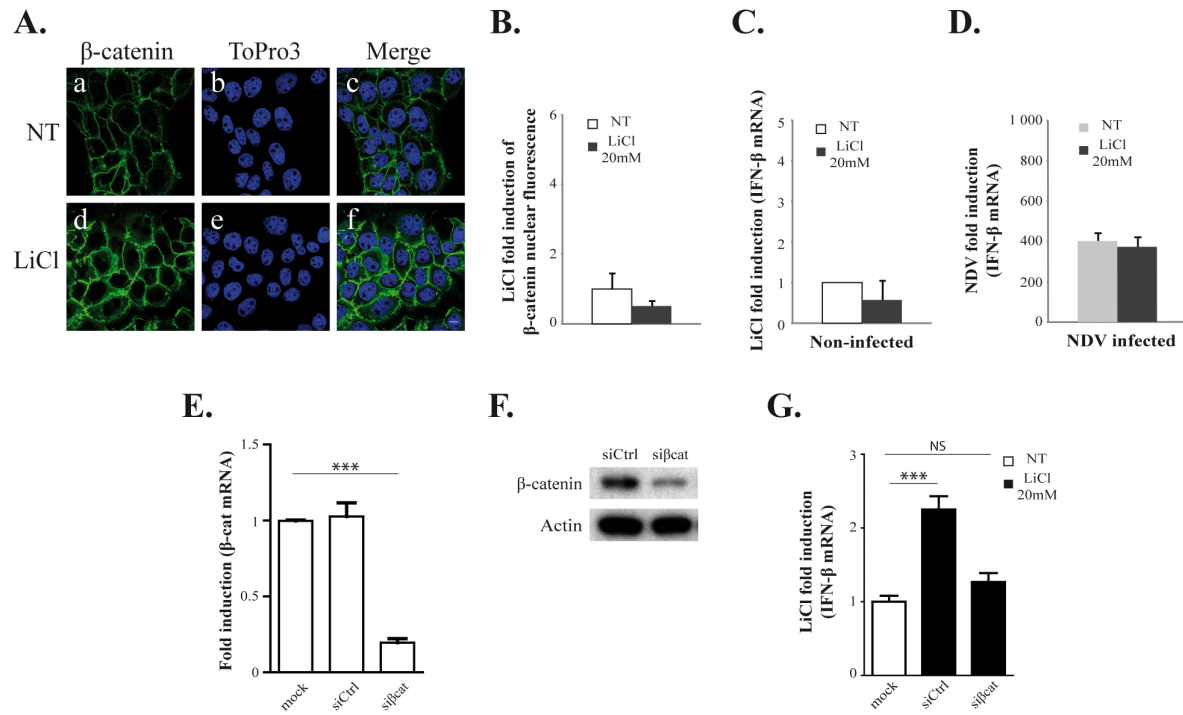
Figure 2. LiCl enhancement of IFN-β expression is mediated by β-catenin. (**A**-**D**) AML12 cells were either non-treated (NT) or treated with 20mM LiCl (LiCl) during 24h and either non-infected (**A**-**C**) or NDV-infected (**D**). (**A** and **B**) Cells were labeled with an anti-β-catenin antibody (a, d) and a DNA intercalating agent to visualize the nucleus (ToPro3; b, e). Nuclei were outlined as shown in merge images (c, f), and total green pixel intensity corresponding to β-catenin labeling in the nucleus was quantified (**B**). IFN-β mRNA (**C** and **D**) was analyzed by RT-qPCR in non-infected (**C**) and NDV-infected (6h p.i.) (**D**) cells either non-treated (NT) or pre-treated with LiCl (LiCl). The corresponding fold inductions were calculated with respect to non-treated (**C**) or non-infected and non-treated (**D**) cells. (**E**-**G**) L929 cells were either mock-transfected (mock) or transfected with β-catenin specific (siβcat) or control (siCtrl) siRNA for 72h. β-catenin mRNA (**E**) and protein level (**F**) were analyzed by RT-qPCR and WB respectively. (**G**) Post-siRNA, cells were either non-treated (NT) or treated with 20mM LiCl (LiCl) during 24h before being NDV-infected. IFN-β mRNA was analyzed by RT-qPCR (**E** and **G**) the corresponding fold inductions were calculated with respect to mock-transfected, non-treated and NDV-infected cells (n=3). Student test: p-value less than 0.001 (***) and 0.01 (**). All images correspond to one confocal section. Scale bar = 10μM.
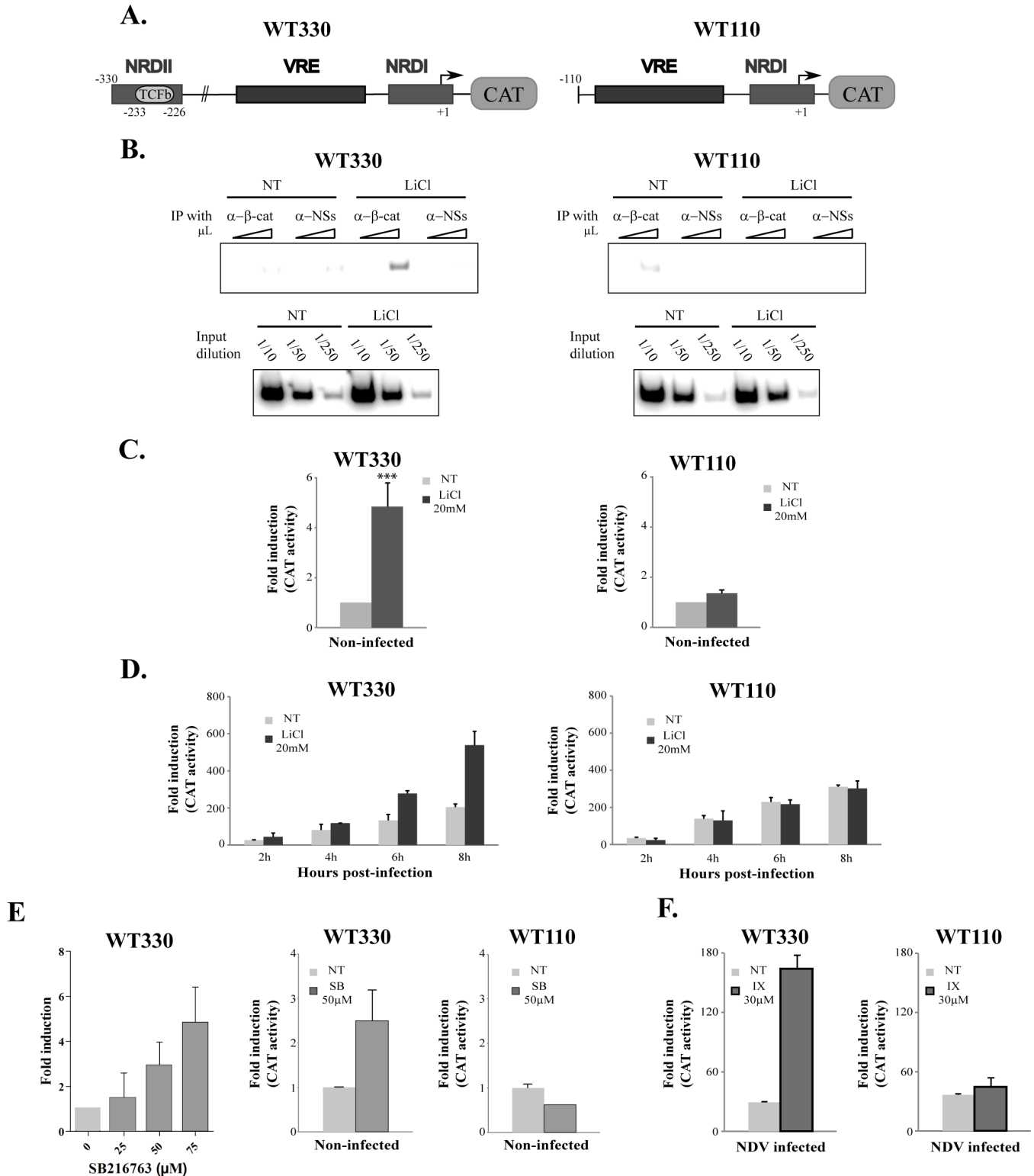
Figure 3. Interaction of β-catenin with the IFN-β promoter region containing a TCF binding site is necessary for LiCl enhancement of IFN-β promoter activity. (**A**) Schematic representation of the WT330 and WT110 murine IFN-β promoters fused to the CAT reporter gene and integrated into the genome of L929 WT330 and L929 WT110 cell lines respectively. (**B** to **D**) β-catenin binding to WT330 and WT110 promoters and corresponding CAT activities were analysed in L929 WT330 and WT110 cells either non-treated (NT) or treated with LiCl 20mM (LiCl). (**B**) Genomic DNA was collected 24h post-LiCl treatment and immunoprecipited with anti β-catenin (α-β-cat) or anti NSs (α-NSs, negative control) antibodies. Increasing amounts of immunuprecipitated DNA (IP), as well as non immunoprecipitated genomic DNA (Input) were amplified by semi-quantitative PCR using specific primers for the WT330 and WT110 integrated promoters. (**C**) Cells were collected post-LiCl treatment and their CAT activities quantified. The corresponding fold inductions were calculated with respect to non-treated cells (n=12 for WT330 and n=6 for WT110 cell lines). (**D**) Post-LiCl treatment, cells were further mock- or NDV-infected, collected at different times post-infection and the corresponding CAT activities were quantified. The corresponding fold inductions were calculated with respect to non-infected non-treated cells (n=4). (**E** and **F**). CAT activities of L929 cells either non-treated (NT) or treated with 50μM of SB 216763 (**E**) or 30μM of IX inhibitor during 24h. (**F**). Cells were further mock or NDV-infected, collected 8h post-infection and the corresponding CAT activities quantified. The corresponding fold inductions were calculated with respect to non-infected non-treated cells.
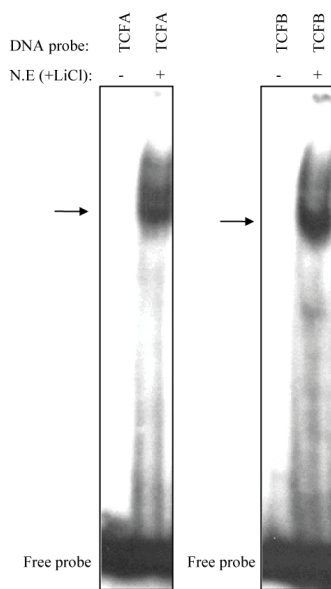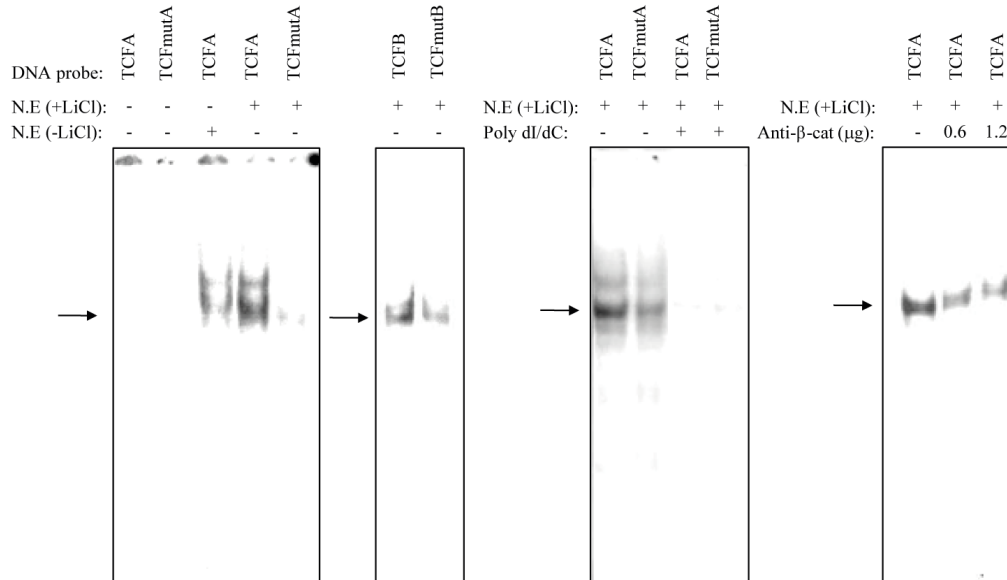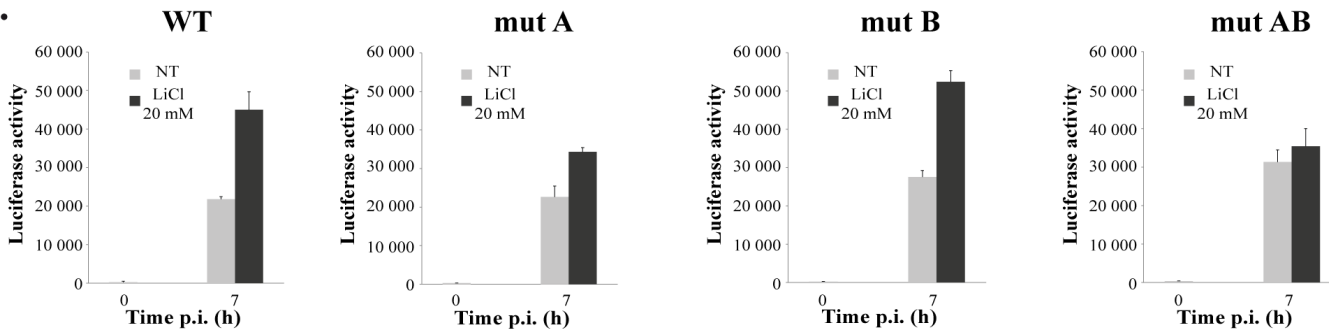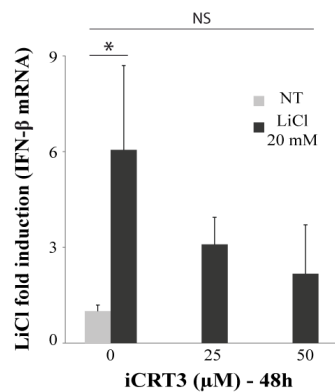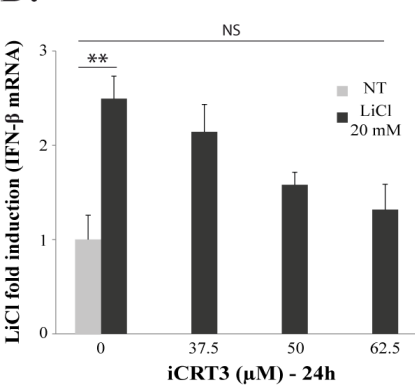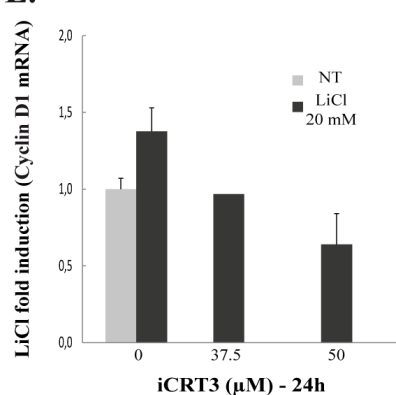
Figure 4. TCF binding sites mediate LiCl-dependent activation of the IFN-β promoter. (**A and B**) Equal amounts of nuclear extracts (N.E) prepared from L929 either non-treated (-LiCl) or treated with 20mM LiCl (+LiCl) during 24h were incubated with the radioactively labeled probes corresponding to wild type TCFa (TCFA) and TCFb (TCFB) or mutated TCFa (TCFmutA) and TCFb (TCFmutB) sites. When indicated, nuclear extracts were incubated with 500ng of poly dI/dC or anti-β-catenin antibodies before adding the probes. (**C**) L929 cells transfected with plasmids containing luciferase reporter gene under the control of the IFN-β promoter either WT or mutated at the TCFa site (mutA), the TCFb site (mutB) or the TCFa and b sites (mutAB) were either non-treated (NT) or pre-treated with LiCl (LiCl) before infection with NDV. Cells were collected 7h p.i. and the luminescence was quantified with n=3. (**D and E**) L929 cells were either non-treated (NT) or treated with 20mM LiCl (LiCl) during 24h or 48h in the presence or absence of iCRT3 before being NDV-infected. IFN-β (**D**) or cyclin D1 (**E**) mRNA was analyzed by RT-qPCR and the corresponding fold inductions were calculated with respect to non-treated NDV-infected (**D**) or non infected (**E**) cells; in D (n=3).
Student test: p-value less than 0.01 (**) and 0.05 (*).
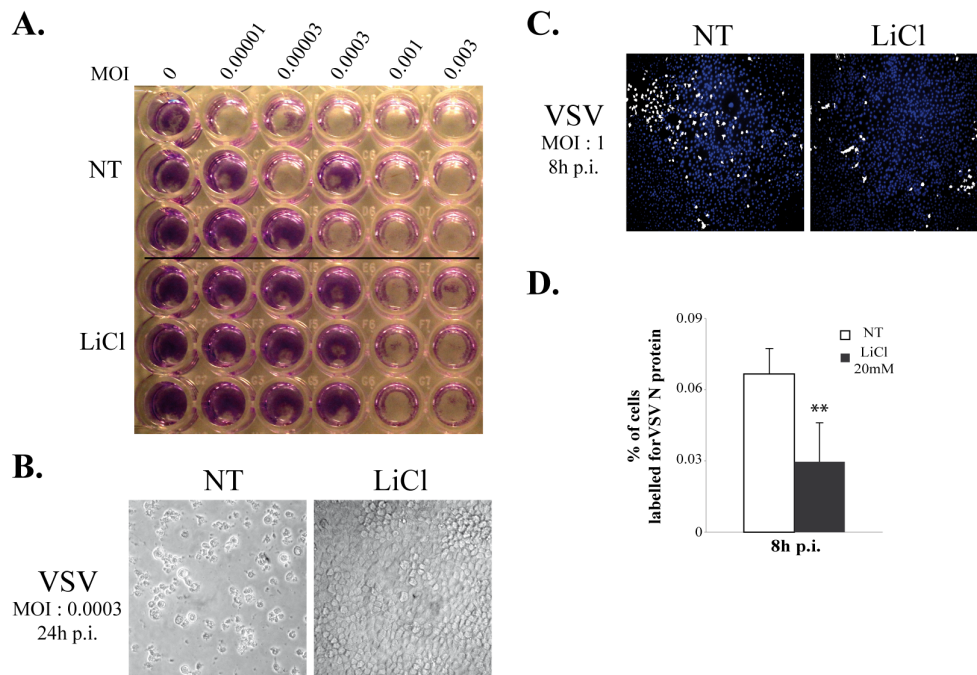
A.

C.

B.

D.

Figure 5. LiCl treatment confers an antiviral state. Monolayers of L929 cells either non-treated (NT) or pre-treated with LiCl 20mM for 24h were infected with VSV. (**A**) Cytopathic effect induced by increasing MOI of VSV was assayed by crystal violet dye staining 24h after infection; (**B**) Photographs of typical culture fields. (**C** and **D**) Cells were fixed 8h after infection (MOI=1), labeled with an antibody directed against the N protein of VSV (displayed in gray) and ToPro3 (blue); merge images of the corresponding culture fields are displayed in (**C**). The % of infected cells, as determined by the presence of N protein encoded by VSV (fluorescence displayed in gray) was determined from a total of 7876 untreated and 9024 LiCl-treated cells counted with n = 4 (**D**).
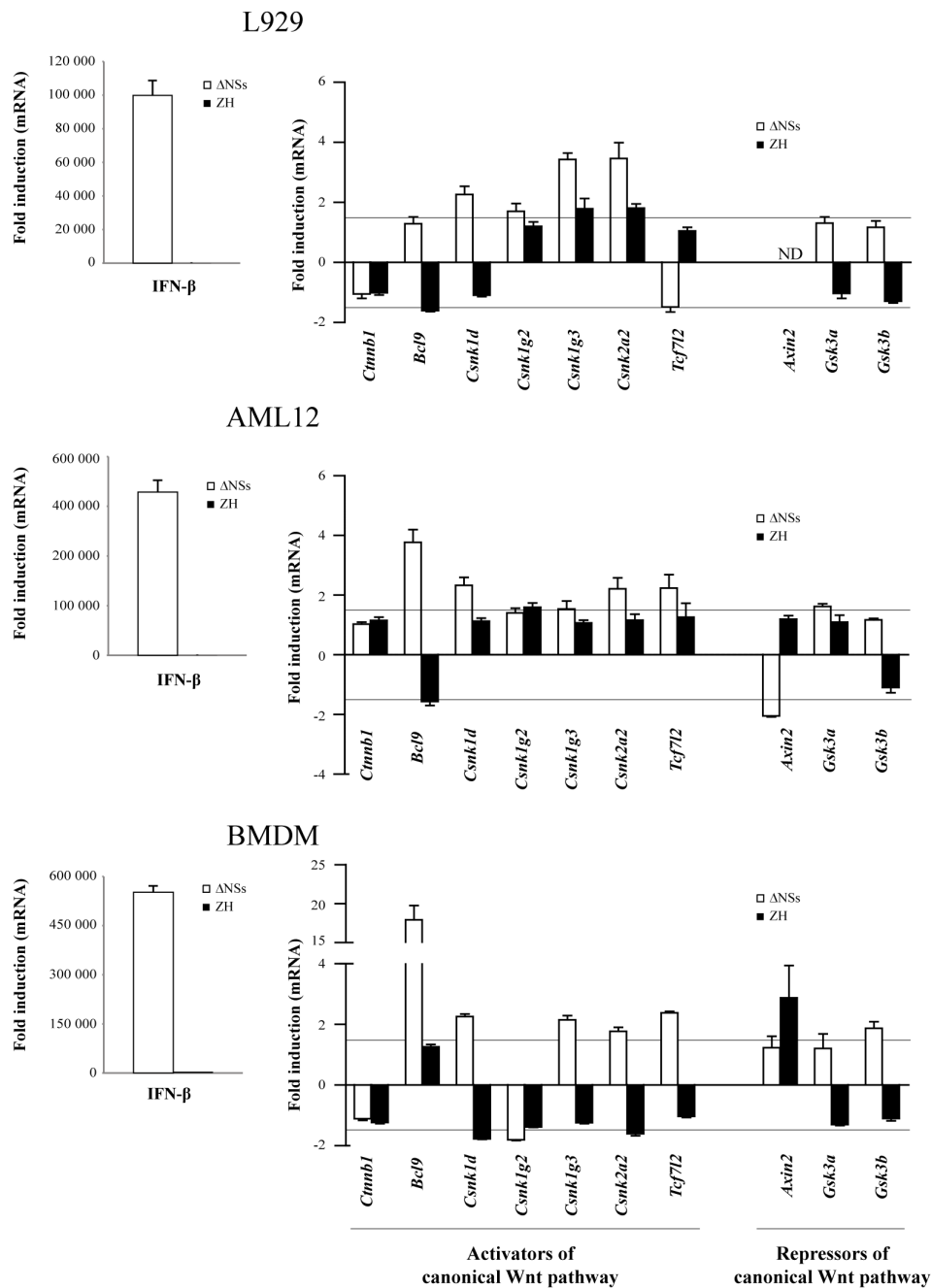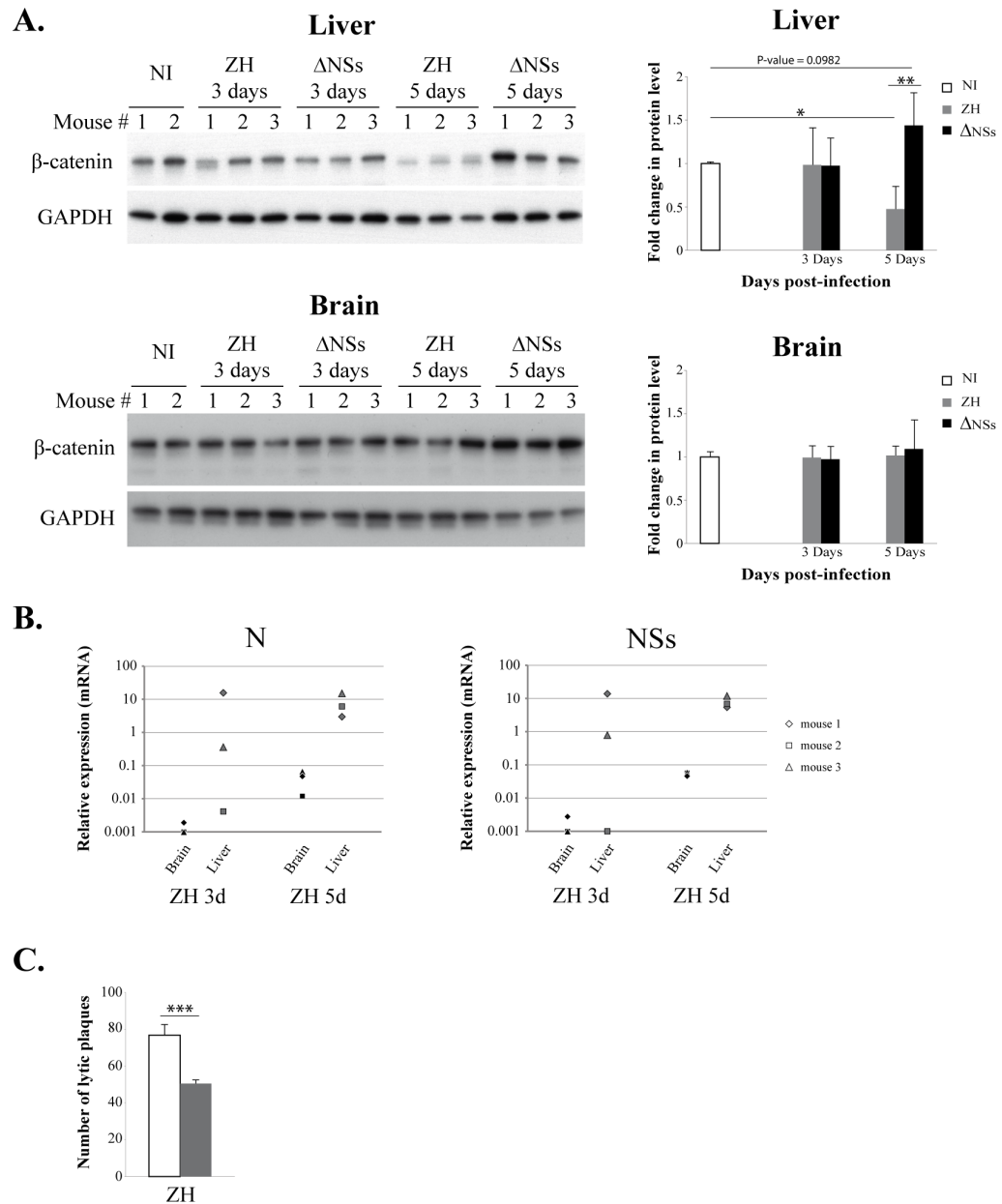
Figure 6. Infection with RVFV affects the Wnt/β-catenin pathway at the transcriptional level.
The expression of genes associated to the Wnt/β-catenin pathway previously identified as interacting
with the NSs protein of RVFV (listed in Table II) was measured in three different cell types corresponding
to fibroblast (L929), hepatocytes (AML12) and Bone Marrow Derived Macrophages (BMDM) either
mock-, RVFZH548- (ZH) or RVFVΔNSs- (ΔNSs) infected. RNAs purified from mock- or virus-infected
cells (8h p.i.) were analyzed by RT-qPCR with primers specific for each gene of interest. The change in gene expression
was calculated in ZH and ΔNSs-infected cells with respect to mock-infected cells. The horizontal broken lines indicate
the cutoff value for upregulation (+1.5 fold) and downregulation (-1.5 fold). The effect of virus infection upon the expression
of genes coding for WNT ligands as well as for antagonist of Wnt signaling (Apcdd1, Dkk1 and Kremen2) could not be tested
since the corresponding mRNA remained undetectable in the three cell types analyzed here. n≥3 for each cell line.
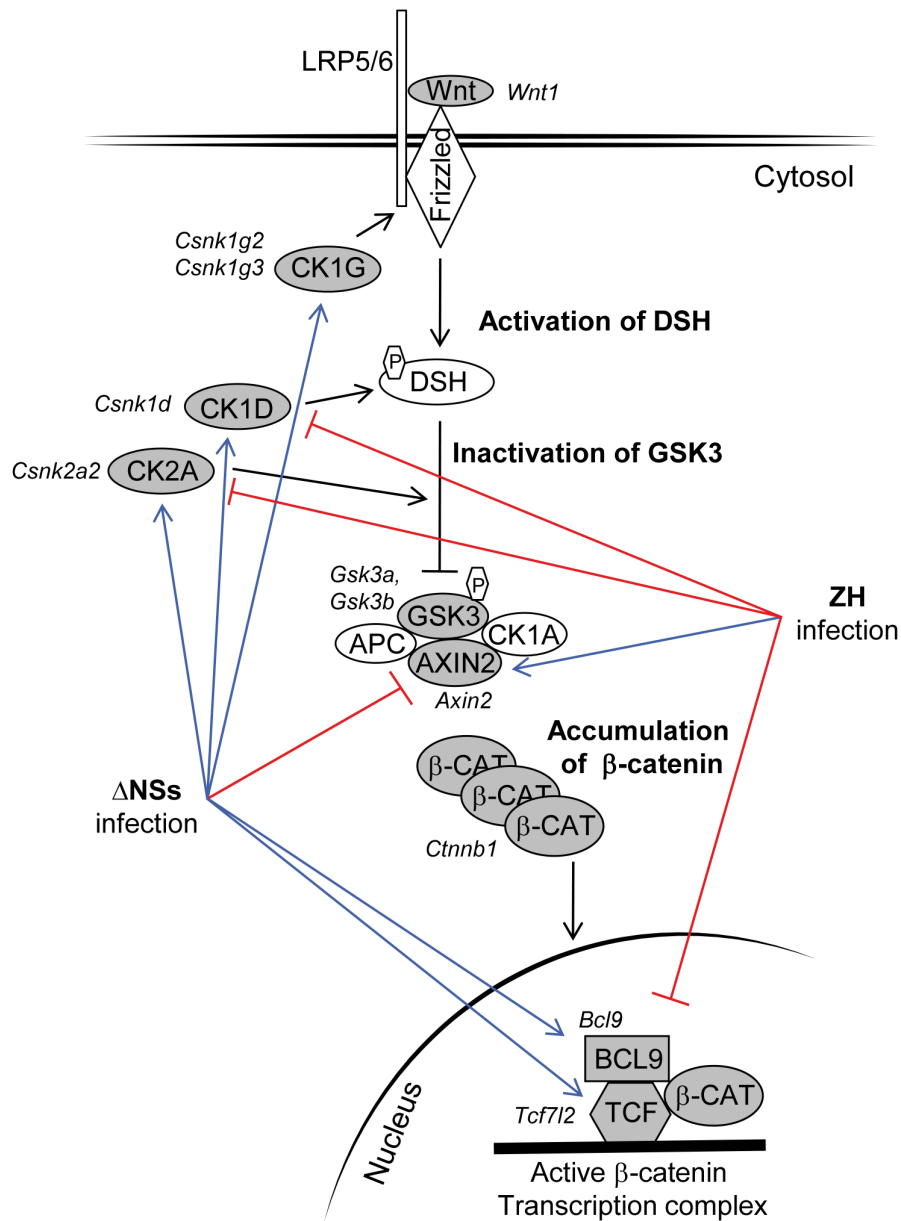
Figure 7. Non-pathogenic and pathogenic strains of RVFV have opposite effects on the Wnt/β-catenin pathway. Genes participating in the Wnt/β-catenin pathway whose promoter regions were identified as significantly interacting with RVFV NSs protein during ChIP-on-chip experiments, listed in Table II, are shown in gray. Genes whose expressions were affected after infection with either the non-pathogenic ΔNSs or the pathogenic ZH strain of RVFV with respect to mock-infected cells are indicated by blue (upregulated) or red (downregulated) arrows.

Figure 8. A physiological relevance for β-catenin protein level during RVFV infection. (**A** and **B**) β-catenin protein and viral N and NSs RNA levels were evaluated in liver and brain of mice either non-infected (NI) or at days 3 and 5 p.i. with RVFVZH548 (ZH) or RVFVΔNSs (ΔNSs). (**A**) β-catenin protein level was analysed by Western blot and estimated densitometrically by comparison with the band intensity of GAPDH; fold changes in protein level were calculated by comparison of the relative β-catenin level in infected versus non-infected (NI) samples. Values were averaged from (n) independent samples per time point with n=3 mice (NI), n=6 mice (ZH 3 days and ΔNSs 3 and 5 days) and n=4 mice (ZH 5 days). (**B**) The relative level of viral N and NSs mRNA were estimated by comparison with the expression of three reference genes (Ppib, Hprt1 and Utp6c). (**C**) Number of lytic plaques formed in monolayers of L929 cells either non-treated or pre-treated with LiCl 20 mM during 24h and infected with RVFVZH548. Cells were fixed and stained with crystal violet 3 days p.i. (n=4). Student test: p-value less than 0.001 (***) 0.01 (**) and 0.05 (*).